PB84-168913

Studies of Particulate Removal from Diesel Exhaust

Southern Research Inst., Birmingham, AL

Prepared for

Industrial Environmental Research Lab.
Research Triangle Park, NC

Mar 84

U.S. Department of Commerce
National Technical Information Service
NTIS

PB84-168913

EPA-600/7-84-029
March 1984

STUDIES OF PARTICULATE REMOVAL FROM DIESEL EXHAUST

by

M. G. Faulkner, J. L. DuBard, J. R. McDonald
Southern Research Institute
2000 Ninth Avenue, South
Birmingham, AL 35255

Contract No. 68-02-3118

Project Officer: D. C. Drehmel
Industrial Environmental Research Laboratory
Research Triangle Park, NC 27711

Prepared for:

U.S. Environmental Protection Agency
Office of Research and Development
Washington, DC 20460

INDUSTRIAL ENVIRONMENTAL RESEARCH LABORATORY
OFFICE OF RESEARCH AND DEVELOPMENT
U.S. ENVIRONMENTAL PROTECTION AGENCY
RESEARCH TRIANGLE PARK, NC 27711

REPRODUCED BY
NATIONAL TECHNICAL
INFORMATION SERVICE
U.S. DEPARTMENT OF COMMERCE
SPRINGFIELD, VA. 22161

TECHNICAL REPORT DATA
(Please read Instructions on the reverse before completing)

1. REPORT NO. EPA-600/7-84-029	2.
3. RECIPIENT'S ACCESSION NO. PB84 168913	
4. TITLE AND SUBTITLE Studies of Particulate Removal from Diesel Exhaust	5. REPORT DATE March 1984
	6. PERFORMING ORGANIZATION CODE
7. AUTHOR(S) M.G.Faulkner, J.L.DuBard, and J.R.McDonald	8. PERFORMING ORGANIZATION REPORT NO. SoRI-EAS-81-268
9. PERFORMING ORGANIZATION NAME AND ADDRESS Southern Research Institute 2000 Ninth Avenue South Birmingham, Alabama 35225	10. PROGRAM ELEMENT NO.
	11. CONTRACT/GRANT NO. 68-02-3118
12. SPONSORING AGENCY NAME AND ADDRESS EPA, Office of Research and Development Industrial Environmental Research Laboratory Research Triangle Park, NC 27711	13. TYPE OF REPORT AND PERIOD COVERED Final; 5/78-4/81
	14. SPONSORING AGENCY CODE EPA/600/13

15. SUPPLEMENTARY NOTES IERL-RTP project officer is Dennis C. Drehmel, Mail Drop 4, 919/541-7505. For details, contact W.B. Kuykendal, Mail Drop 61 919/541-7865.

16. ABSTRACT The report gives results of a characterization of the collection of particulate emissions from diesel exhaust by several different methods, using 5.7 liter GM diesel engines (as sources) and such controls as fiber and gravel bed filters, trap/cyclones, and ESPs. Overall and fractional mass collection efficiencies and operating characteristics of the controls were determined by inlet and outlet total mass loading measurements and particle size distributions. A fiber filter--with long fiber glass wool, batts of fiberglass insulation, and stainless steel fiber mats--showed collection efficiencies as high as 90% with a quick pressure rise culminating in gas sneakage. A gravel bed filter of 45.7 cm diameter and 10.2 cm depth with 2 mm steel shot showed efficiencies of 45-70% and increasing with increasing system backpressure. A two-stage ESP, used to agglomerate the primary particulate matter, resulted in an order-of-magnitude increase in mass median diameter. An ESP/cyclone combination provided a collection efficiency of at least 50%. Methods of cleaning the control devices and removing collected particulate are discussed.

17. KEY WORDS AND DOCUMENT ANALYSIS

a. DESCRIPTORS	b. IDENTIFIERS/OPEN ENDED TERMS	c. COSATI Field/Group
Pollution Diesel Engines Exhaust Gases Dust Aerosols Filters Fibers Gravel Cyclone Separators Electrostatic Separators	Pollution Control Particulate	13B 11E 21G 13C 21B 13I,07A 11G 07D 14G

18. DISTRIBUTION STATEMENT Release to Public	19. SECURITY CLASS (This Report) Unclassified	21. NO. OF PAGES 106
	20. SECURITY CLASS (This page) Unclassified	22. PRICE

EPA Form 2220-1 (9-73)

NOTICE

This document has been reviewed in accordance with U.S. Environmental Protection Agency policy and approved for publication. Mention of trade names or commercial products does not constitute endorsement or recommendation for use.

ABSTRACT

A series of tests has been conducted to characterize the collection of particulate emissions from diesel exhaust by several different methods. The sources of particulate emissions were 5.7 liter GM diesel engines. The control devices which are discussed include fiber filters, gravel bed filters, trap/cyclones, and electrostatic precipitators (ESP). The overall mass collection efficiencies, fractional mass collection efficiencies, and operating characteristics of these devices were determined by measurements of inlet and outlet total mass loadings and particle size distributions.

A device containing a fiber filter was investigated with three different filter materials: long fiber glass wool, batts derived from fiberglass insulation, and stainless steel fiber mats. Collection efficiencies as high as 90% were achieved, coupled with a quick pressure rise culminating in gas sneakage. A device containing a gravel bed of 45.7 cm diameter and 10.2 cm depth was investigated with 2 mm steel shot. Efficiencies ranged from 45 to 70% and increased with increasing system backpressure.

A two-stage ESP was used to agglomerate the primary particulate matter, resulting in an order-of-magnitude increase in mass median diameter. The agglomerated particulate is characterized. Aerosol sampling data are presented for the variation in particle size distribution and the efficiency of trapping the agglomerated particulate in cyclones, fiber filters, and a granular bed filter. The ESP/cyclone combination can provide a collection efficiency of at least 50%. Overall mass removal efficiencies greater than 80% have been achieved with an ESP/granular bed filter system for a duty distance greater than 800 km (500 miles) at a constant highway speed of 88 km/hr (55 mph). Methods of cleaning the devices and removing collected particulate are discussed.

CONTENTS

Abstract..... iii
Figures..... v
Tables..... viii
Acknowledgements..... ix

1. Introduction..... 1
2. Conclusions..... 3
3. Recommendations..... 5
4. Gas Stream Sampling Techniques..... 6
   - Summary of Measurements Made..... 6
   - Measurement Techniques..... 14
5. Mechanical Devices..... 26
   - Deep Bed Filter..... 26
   - Gravel Bed Filter..... 35
   - Condensation Traps..... 45
   - Ceramic Barrier Filter..... 54
   - Cooled Exhaust Line..... 58
6. Electrostatic Precipitators..... 60
   - Cylindrical Electrostatic Precipitator..... 60
   - Diesel Particulate Resistivity..... 64
   - ESP Cleaning Fluids..... 64
   - Moving Belt Electrostatic Precipitator..... 66
7. Combined Electrical and Mechanical Devices..... 74
   - Electrified Filter..... 74
   - ESP/Cyclone Combinations..... 77
   - ESP/Gravel Bed Filter Combination..... 83
   - ESP/Deep Bed Filter Combination..... 89
8. Design of an Aftertreatment Device..... 91

References..... 93
Glossary..... 95

FIGURES

1	Initial diesel exhaust test configuration.....	7
2	Final diesel exhaust test configuration with axial sampling ports.....	8
3	Diesel exhaust test configuration used at DOT.....	9
4	Cumulative percentage by mass for diesel engines used at DOT and SoRI.....	11
5	Cumulative mass loading for diesel engines at DOT and SoRI.....	12
6	Differential mass concentration for diesel engines used at DOT and SoRI.....	13
7	Operation principle and typical performance for a cascade impactor.....	16
8	University of Washington Mark III source test cascade impactor.....	17
9	Modified Southern Research Institute SEDS.....	22
10	Theoretical dilution versus actual dilution for 0.15 μm particles in the SoRI diluter.....	23
11	SoRI diluter, cut-away view.....	24
12	Deep bed filter.....	27
13	Pressure drop across fiber glass batt (11/14/79).....	29
14	Fiberglass batts with accumulated soot.....	30
15	Efficiencies before and after onset of sneakage for deep bed filter using fiberglass batts (11/14/79)....	31
16	Pressure drop across glass wool (11/12/79).....	33
17	Pressure drop across glass wool (11/13/79).....	34
18	Damaged area on stainless steel filter (5/22/80).....	36

19	Pressure drop across fiberglass batt (11/15/79).....	38
20	Efficiency for deep bed filter using 15 cm of glass wool (11/12/79).....	39
21	Pressure drop across deep bed filter with steel fiber mat (5/7/80).....	40
22	Pressure drop across deep bed filter with steel fiber mat (5/8/80).....	40
23	Efficiency for deep bed filter using stainless steel filter mat (5/8/80).....	41
24	Pressure drop across steel fiber mat (5/22/80).....	42
25	Gravel bed filter efficiency and backpressure.....	44
26	Gravel bed filter backpressure with stirring.....	46
27	Gravel bed filter output with stirring at 30 minute intervals.....	47
28	Cross section and relative sizes of medium and large capacity Aut-Ainers.....	49
29	Flat condensation trap.....	51
30	Aut-Ainer efficiency for 88 and 48 kph speeds.....	53
31	Gas chromatogram of residue from filters taken during the large Aut-Ainer test.....	55
32	Pressure drop across Corning ceramic filter (DOT data, 5/9/80).....	57
33	Hydrocarbon condensation on diesel soot as a function of temperature.....	59
34	Schematic diagram of the precipitator.....	61
35	Removal of diesel particulate from small size ranges by electrostatic precipitation.....	63
36	Moving belt electrostatic precipitator.....	68
37	IV curves for moving belt electrostatic precipitator.	70
38	Efficiency of the moving belt precipitator for the small particles.....	72

39	Schematic diagram of the electrified filter.....	75
40	Impactor testing of ESP/cyclone combination. Cumulative percent particulate mass of aerodynamic diameter less than the impactor stage D_{50} cutpoints..	79
41	Impactor testing of ESP/gravel bed combination. Cumulative percent particulate mass of aerodynamic diameter less than the impactor stage D_{50} cutpoints..	80
42	Impactor testing of ESP/gravel bed combination. Cumulative percent particulate mass of aerodynamic diameter less than the impactor stage D_{50} cutpoints..	84
43	Impactor testing of ESP/gravel bed combination. Cumulative percent particulate mass of aerodynamic diameter less than the impactor stage D_{50} cutpoints..	85
44	Mass removal efficiency in small size ranges of diesel particulate.....	87
45	Schematic diagram of prototype diesel exhaust cleaning device. Minimum collection efficiency 70%. Overall length 0.84 m (33 in.).....	92

TABLES

1	Summary of Deep Bed Filter Tests.....	37
2	Summary of Gravel Bed Filter Tests.....	48
3	Summary of Condensation Trap Tests.....	56
4	Diesel Particulate Resistivity.....	65
5	Effectiveness of Diesel Soot Flushing Fluids.....	67
6	Cumulative Percent Mass > D_{50} of Diesel Soot Agglomerated by the ESP.....	81
7	Summary of Testing Small Cyclones at High Gas Flow Rates.....	82
8	Total Mass Loadings Measured for the ESP/Gravel Bed Combination.....	86
9	Mass Removal Efficiency of the ESP in Combination with 20 cm Diameter Gravel Bed Filter.....	89

ACKNOWLEDGEMENTS

The cooperation and assistance of the personnel of the Department of Transportation, Transportation Systems Center, Cambridge, Massachusetts, is greatly appreciated. Thanks are also expressed to the personnel of the Physics Division of Southern Research Institute for their help with the data acquisition.

SECTION 1

INTRODUCTION

The superiority in fuel economy of the diesel engines compared to a gasoline engine of the same horsepower has created a widespread market for diesel powered light duty vehicles due to the increasing cost of fuel. In addition, automobile manufacturers view the diesel engine as a possible solution to the Federal Government's regulation requiring that the average fuel mileage for each auto manufacturer be at least 11.6 Km/l. (27.5 mi/gal.) by the year 1985. Unfortunately, one characteristic of the diesel engine is a high level of combustion by-products, the most obvious of which is particulate matter.*

The particulate effluent of the diesel engine consists largely of agglomerates of very small particles of carbon which have condensed hydrocarbons adsorbed onto them. The amount of adsorbed hydrocarbons present on the soot particles is a function of temperature and increases as the soot passes from the very hot engine through the exhaust system to the relatively cool environment outside of the car. An analysis of the collected particulate matter indicates that 33 to 50% is composed of organic substances.[1] Among these substances are many polynuclear aromatic compounds, including the highly carcinogenic benzo(a)pyrene, which is often used as an indication of the potential health danger of exhaust products. Although the benzo(a)pyrene concentration of light duty diesel engines is equivalent to that of noncatalyst gasoline engines, it is an order of magnitude greater than the levels found in catalyst-equipped gasoline engines. The biological hazard is enhanced by the small size of the particles. The mass median diameter (mmd) of the soot ranges from 0.3 to 0.5 μm with about 70% less than 1 μm.[2] Suspension times for particles of this size may be measured in days.[3] Since these particles fall into the respirable size range, the suspension time is directly related to the exposure time for human beings and therefore to the chance of absorption of such substances as benzo(a)pyrene by the body.

---

*EPA has defined particulate matter as everything collected on a fluorocarbon coated glass fiber filter at 52°C (125°F) after dilution with ambient air in a dilution tunnel.

The small size of the particulate matter places it in a range where the collection efficiency of both filtration and electrostatic devices is reduced. The problem of particle collection is magnified by the large quantities of particles produced, amounts ranging from 0.14 g/km for the Volkswagon Rabbit to 0.53 g/km for the General Motors 5.7 liter engine.[4] The ultimate goal for particulate emissions set by EPA is 0.125 g/km,[4] which would require that 76% of the particulate matter from the GM 5.7 liter engine be removed from i exhaust stream. Over an 8000 km (5000 mile) service interval, this would amount to about 3.2 kg of soot. Using 120 kg/m^3 for the value of the bulk density for this collected material,[1] this amounts to about 27 liters ($\sim$1 ft^3).

In order to aid in the development of a solution to the diesel emission problem, EPA is supporting research programs to investigate several approaches to particulate reduction. As one of these programs, Southern Research Institute (SoRI) has been studying non-regenerative after-treatment devices for the collection of diesel particles. These include both devices which have been specifically developed for light duty vehicles and stationary source-type devices which have been adapted to vehicular sources. The devices tested fall in the categories of mechanical, electrostatic, and combination electrical/mechanical devices. The mechanical devices include a deep bed filter which can accommodate up to a 15 cm depth of fibrous filter material, a granular bed filter, and a barrier filter. Also in this category are condensation traps which depend on gas stream cooling to condense particulate matter on a relatively coarse wire mesh.

There were two electrostatic devices tested. One was a two-stage electrostatic precipitator (ESP) which featured wet flushing and concentric cylinders for collection surfaces.[5] The other device was a moving belt ESP designed for diesel particulate control. In this device the collection surface is a thin steel belt which slowly moves so that the collected material is removed from the area of high gas flow to reduce reentrainment.

The combination electrical/mechanical device category included an electrified filter[5] and several mechanical devices used in conjunction with the two-stage ESP. The electrified filter was a two-stage radial flow precipitator which has a nonconductive fiber filter mat located between the collection electrodes. The devices coupled with the ESP were used in an attempt to take advantage of the agglomeration effect provided by the ESP. These devices were cyclones of various configurations, the deep bed filter and the granular bed filter.

The test results of the devices examined in this program are described in depth in Sections 5, 6, and 7 of this report. Section 4 describes the test layout and particle sampling techniques used. The design of a prototype collection device is presented in Section 8.

SECTION 2

CONCLUSIONS

The use of a fine fiber filter to capture diesel soot particles does not appear to be practical due to the tendency toward formation of a cake on the face of the filter. This cake of collected soot reduces the gas flow through the filter which results in an increase in the pressure drop across the device. The pressure continues to increase until either it impedes the operation of the engine or a lower pressure route around the filter mat is established. Once a route for gas sneakage is established, the collection efficiency of the device drops sharply. This effect was noticeable in both the purely mechanical and in the electrified filters. In addition, the electrified filter showed electrical deterioration due to the accumulation of soot on the insulators.

The ceramic filter proved to be highly effective but is subject to the same limitation as the fine fiber filters. However, since this material was designed as a catalytic substrate, it may be possible to regenerate the device periodically thereby greatly extending its usable lifetime. Development of the device with this goal in mind is being undertaken by EPA at Ann Arbor, Michigan as well as by several automobile manufacturers.

The three condensation traps tested were unable to achieve acceptable collection efficiency levels. In addition, there was no evidence that these devices were agglomerating particles. Instead, they produced a fog of small particles as hydrocarbon vapors present in the diesel exhaust were condensed in the control device.

The granular bed filter is a concept which may prove applicable to the diesel exhaust problem. Although the collection efficiency was not as high as that of a fiber filter, the granular bed has the important advantage of being cleanable, whether by mechanical agitation or wet flushing. In addition, gas sneakage does not appear to be a problem with this material, possibly due to the fact that it will flow to fit the container.

Neither of the electrostatic precipitators demonstrated high collection efficiencies. The moving belt precipitator (MBP) showed an efficiency of about 21% coupled with poor mechanical

reliability. The cylindrical precipitator (ESP) showed only slightly higher efficiency. However, this device consistently agglomerated the diesel particles by about an order of magnitude. Therefore, the ESP should be given further consideration in combination with some aftertreatment device which is capable of collecting the agglomerated particles.

The collection efficiency of an ESP/gravel bed combination ranged from 86% at a vehicle speed of 88 km/hr to 83% at 24 km/hr in spite of the fact that the particulate mass loading was increased by about 75% at the lower speed. On the other hand, lower exhaust gas flow rates reduce the scouring of the insulating standoffs in the ESP, which in turn reduces the operation time between ESP cleanings. This implies that the periodic cleaning necessary for an ESP agglomerator used on a diesel vehicle may be more frequent for city driving than for long-distance highway driving.

A compact gravel bed filter can be contained within the housing of the ESP, directly below the collecting cylinders, and can achieve a mass removal efficiency of 70%, or better, at acceptable levels of engine backpressure. The gravel bed filter can be cleaned simultaneously with the ESP by wet flushing with a suitable solvent such as percholorethylene.

An ESP agglomerator followed by cyclonic trapping of agglomerated particles is also a viable concept for aftertreatment of diesel exhaust. The mass removal efficiency of such a device is at least 50%. The mass removal efficiency can be improved by extensive engineering and testing to match the cyclone performance to the characteristics of the agglomerated diesel particles.

Methods for disposal of the trapped diesel soot require further investigation. An ESP will require periodic cleaning by wet flushing or air jet scouring. Similarly, a gravel bed will require stirring or wet flushing. Soot collected in a cyclone catchpot will have to be removed and compacted. The frequency of the cleaning is dependent on the type of operation which the vehicle receives. High speed highway driving is expected to require control device maintenance less often than slower in-town operation. However, a suitable cleaning program can only be developed experimentally for a particular vehicle type and control device.

SECTION 3

RECOMMENDATIONS

Fiber filters do not appear suitable for the capture of diesel soot. Fine fiber filters exhibit high collection efficiency but have short lifetimes due to filter blinding. The coarse fiber filters tested, the traps, had inadequate collection efficiency. The granular bed filter proved to be a useable device but needs to be redesigned for adaptation to a vehicle and for easy disposal of collected particles. The ESP's tested demonstrated poor collection efficiencies but proved to be successful particle agglomerators. An ESP in combination with a mechanical collector such as a cyclone or gravel bed may be a useable device but further development is needed to provide a device of practical safety, size and durability as well as to develop the total system for electrode and bed cleaning.

SECTION 4

GAS STREAM SAMPLING TECHNIQUES

SUMMARY OF MEASUREMENTS MADE

The diesel exhaust used for those measurements made at the SoRI laboratory in Birmingham, Alabama was furnished by a 1979 Chevrolet diesel pickup truck powered by a GM 5.7 liter diesel engine. This truck was mounted on a chasis dynomometer installed in a metal building located behind the Environmental Sciences Laboratories building at SoRI. The dual exhaust pipes of the truck were combined and routed out from under the side of the truck for connection to the control devices being tested. Sampling ports were provided in the exhaust lines before and after the control device. At the beginning of the test series, the sampling ports were installed at right angles to the exhaust flow as shown in Figure 1. Later in the test program, when it became necessary to sample isokinetically in order to obtain a more accurate size distribution of the particulate agglomerated by the ESP, the sampling ports were repositioned so they faced directly into the gas flow as shown in Figure 2. This allowed gas extraction without having impaction of the larger particles in the nozzle.

For those tests which were performed at the Department of Transportation (DOT), Transportation Systems Center, in Cambridge, Massachusetts, the exhaust was furnished by a GM 5.7 liter diesel engine which was mounted on an engine dynomometer in one of the test cells at the DOT facility. A plan of one of the test configurations used is shown in Figure 3. All particulate samples obtained by SoRI were extracted at right angles to the exhaust flow. DOT personnel operated and maintained the engine. As part of this task, DOT monitored all vital engine parameters including brake power, torque, RPM, fuel and air consumption, and exhaust temperature and pressure. In addition, DOT sampled the exhaust using their dilution tunnel and measured the levels of hydrocarbons, NO_x, CO, and CO_2 in the diluted gas. DOT also measured the total particulate concentration in the diluted flow using filters.

The majority of the tests were run with the truck operating at a steady road speed of 88 km/hr (55 mph) in order to provide a high load for the control device. At DOT the engine was operated at 1700 rpm to achieve this same condition. This provided

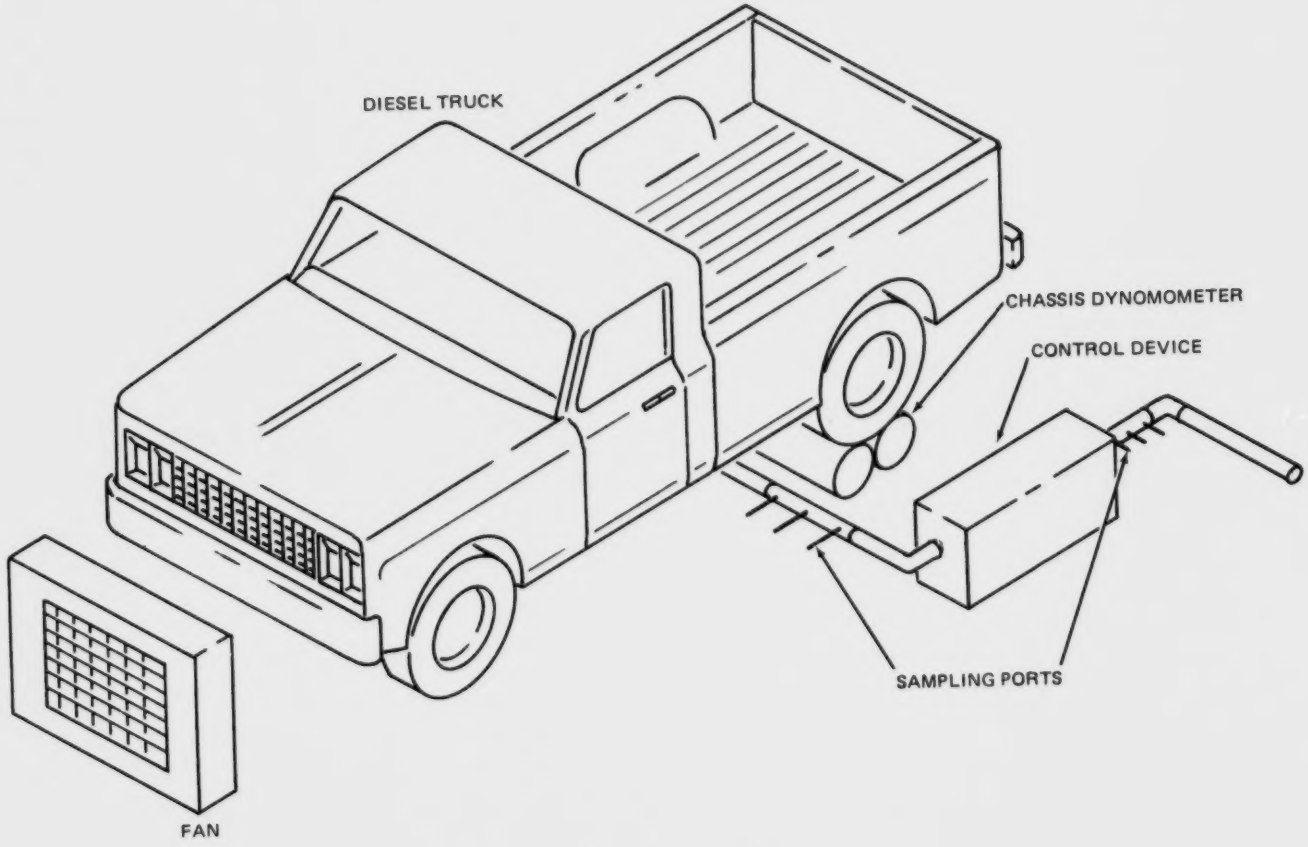

Figure 1. Initial diesel exhaust test configuration.

4181-293

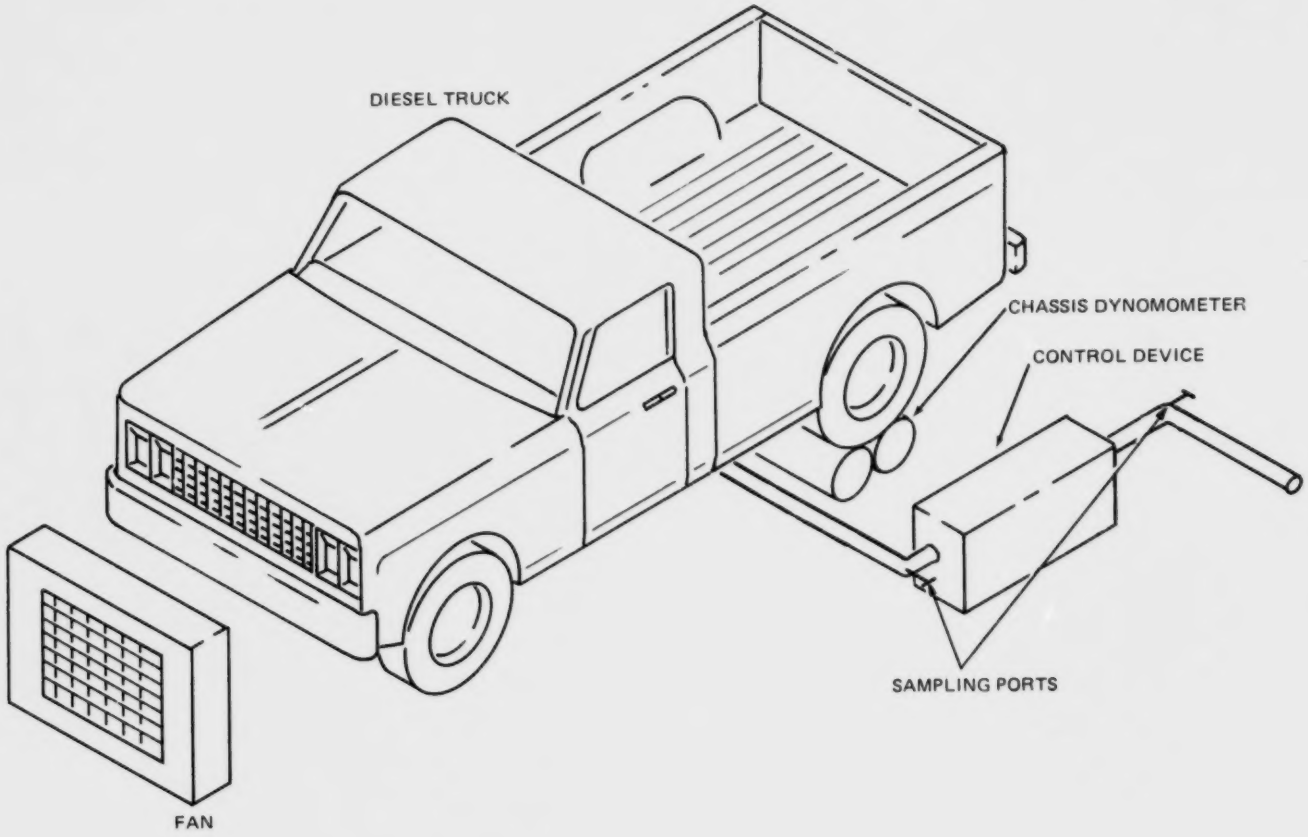

Figure 2. Final diesel exhaust test configuration with axial sampling ports. 4181-294

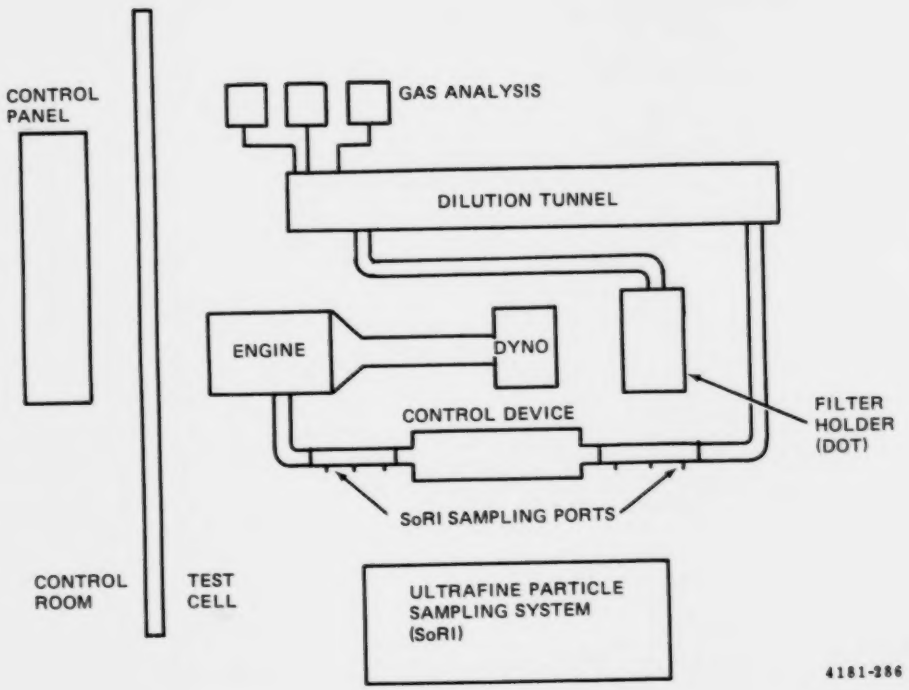

Figure 3. Diesel exhaust test configuration used at DOT.

a gas flow rate of about 7.6 actual m^3/min (270 acfm). For lower speed runs, the truck was run at 24 (15) or 32 km/hr (20 mph). These speeds corresponded to flow rates of 2.4 and 3.2 m^3/min, respectively. The low engine speed used at DOT was 900 rpm corresponding to 48 kph (30 mph). Figures 4, 5, and 6 show 88 km/hr (1700 rpm) size dependent emission data for both the engine used at DOT and the engine used in Birmingham. Figure 4 shows cumulative percentages by mass. Cumulative mass loadings are shown in Figure 5. Figure 6 details the differential mass concentrations for the two engines. The ambient temperatures in Birmingham ranged from 30° (86°) to 46°C (115°F) during the time that these tests were run.

Total mass and particle size distribution measurements were performed before and after each control device undergoing testing in order to characterize the particle collection of the control device. The equipment used were filters, cascade impactors, electrical mobility sizing instruments and optical sizing instruments. Unless otherwise specified, however, the overall mass collection efficiencies quoted are derived from filter data. In addition to these instruments, thermocouples for monitoring the gas stream temperature and mercury and water manometers for monitoring the pressure drop across the control device were used.

Approximate total mass loading information was obtained by using a Gelman 47 mm stainless steel filter holder with glass fiber filters. Filter data can be taken and reduced very quickly, yielding prompt information on particulate concentrations in the gas stream and on particle collection efficiency. The data are also valuable as a check on the data obtained with impactors.

The modified University of Washington Mark V cascade impactors used in these tests were operated using seven stages with stainless steel inserts coated with Apiezon H grease to prevent particle bounce. These instruments were used to obtain particle size distributions on a mass basis over the size range from about 0.2 µm to 4 µm. The impactors were either mounted in ovens close to the exhaust pipe or were wrapped in heating jackets which allowed them to be operated at the same temperature as the exhaust gas. The cut points for the impactor stages occurred at approximately 4.3, 2.2, 1.2, 0.7, 0.4, and 0.2 µm.

A control substrate on which no particle collection took place was run as a part of each impactor sample to monitor the weight stability of the substrates and grease coatings. These controls indicated that the weights of the coated substrates were stable to within about $\pm$0.05 mg. This figure represents ten percent (10%) or less of the individual stage catches in most impactor runs. All weighing of the impactor substrates and back-up filters was done on site after desiccation for a sufficient length of time for the samples to equilibrate. Glass fiber

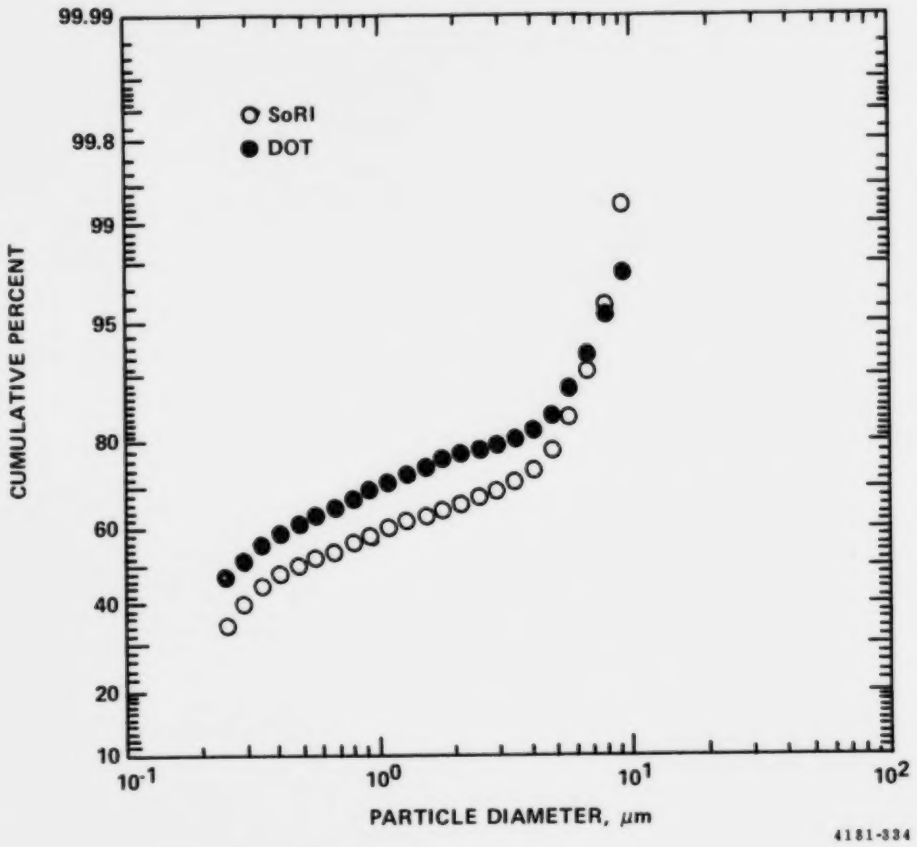

Figure 4. Cumulative percentage by mass for diesel engines used at DOT and SoRI.

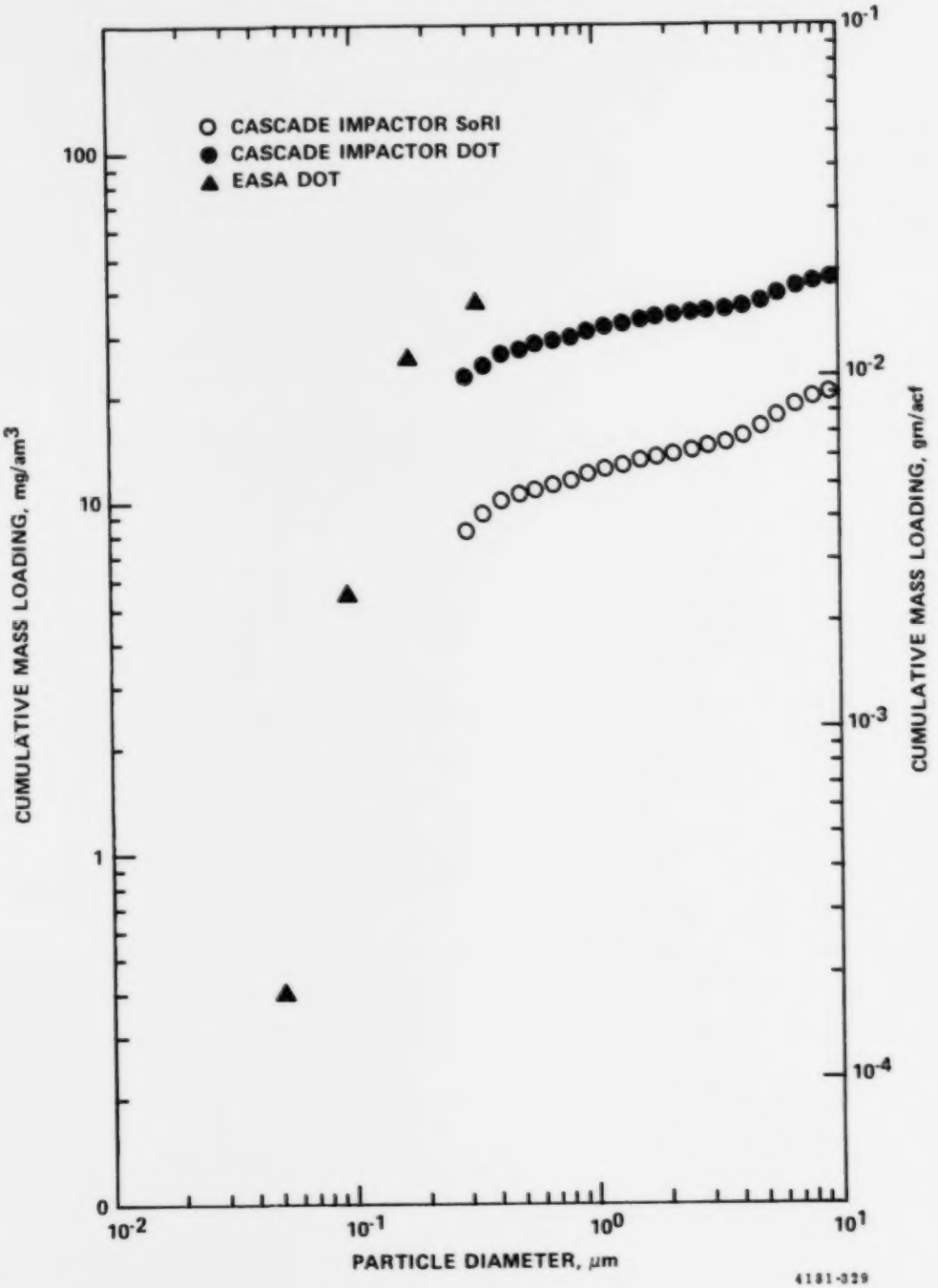

Figure 5. Cumulative mass loading for diesel engines at DOT and SoRI.

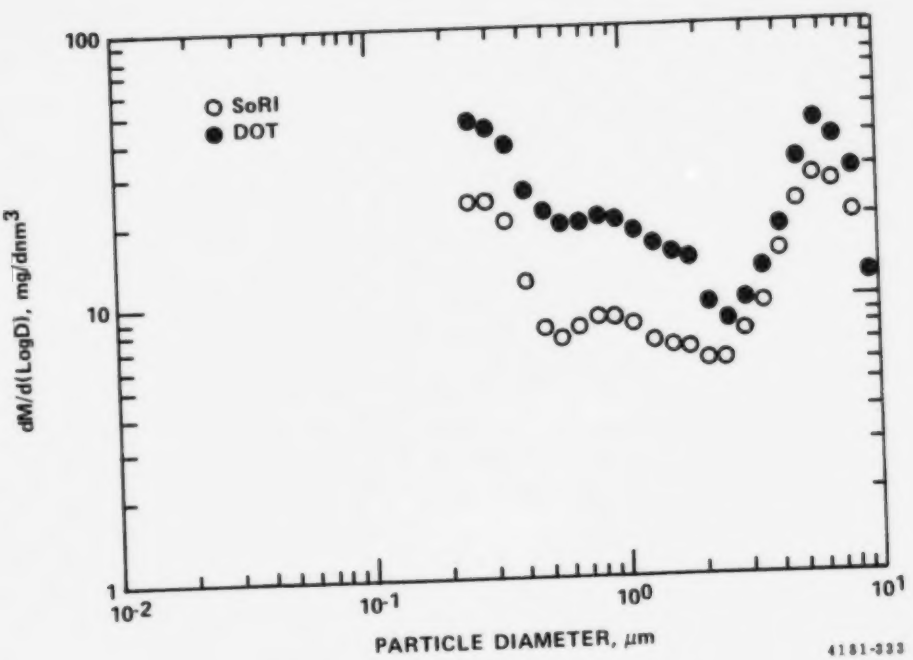

Figure 6. Differential mass concentration for diesel engines used at DOT and SoRI.

material (Reeve Angel 934AH) was washed in sulfuric acid to minimize potential biases which can result from SO_2 uptake by the filters.

In addition to the cascade impactors, a Thermo Systems Model 3030 Electrical Aerosol Size Analyzer (EASA) was used to determine concentrations and electrical mobility derived size distributions of particles in the 0.01 to 0.3 μm size range. A Climet Model 208 optical particle counter was used to monitor concentrations in the fine particle size range. The SoRI SEDS III sample extraction, conditioning, and dilution system was used as an interface between these instruments and the exhaust stream. The system provides a mechanism for the removal of condensable vapors from the sample gas at elevated temperatures followed by controlled dilution to particle concentrations within the operating ranges of the measurement instruments. The optical data were not used for detailed sizing information but provided quick indications of efficiency in several size bands.

MEASUREMENT TECHNIQUES

Inertial Particle Sizing Devices

Two devices which fall into the inertial sizing category are impactors and cyclones. In both of these devices, the aerosol stream is constrained to follow a path of such curvature that the particles tend to move radially outward toward a collection surface because of their inertia. Subsequent analysis of the particle size distribution may be made by gravimetric means, quantitative chemical analysis, or microscopic inspection.

Particle size distribution measurements have largely been made using cascade impactors, which are effective in the size range from 0.2 to 10 μm diameter; although, in some cases, hybrid cyclone-impactor units or cyclones have also been used. The particle size distributions are normally calculated from experimental data by relating the mass collected on various stages to the theoretical or calibrated size cutpoints associated with those stage geometries.

Cascade Impactors--

University of Washington Mark V cascade impactors were used to obtain particle mass and particle size distributions for the diameter range 0.2 to 4 μm.

Because of its compact arrangement and mechanical simplicity, the cascade impactor has gained wide acceptance as a practical means of making particle size measurements in flue gases. In many cases, the impactors can be inserted directly into the duct or flue, eliminating many condensation and sample loss problems which occur when probes are used for extractive sampling.

Figure 7 is a schematic which illustrates the principle of particle collection which is common to all cascade impactors. The sample aerosol is constrained to pass through a slit or circular hole to form a jet which is directed toward an impaction surface. Particles which have lower momentum will follow the air stream to lower stages where the jet velocities are progressively higher. For each stage there is a characteristic particle size which theoretically has a 50% probability of striking the collection surface. This particle size, or D_{50}, is called the effective cut size for that stage. The number of holes or jets on any one stage ranges from one to several hundred depending on the desired jet velocity and total volumetric flow rate. The number of jet stages in an impactor ranges from one to about twenty for various impactor geometries reported in the literature. Most commercially available impactors have between five and ten stages.

Parameters which determine the collection efficiency for a particular geometry are the gas viscosity, the particle density, the jet diameter or width, the jet-to-plate spacing, and the velocity of the air jet.

Most modern impactor designs are based on the semi-empirical theory of Ranz and Wong.[6] More comprehensive theories have been developed by Davies and Aylward[7] and by Marple.[8] In practice, deviations from ideal behavior dictate that the impactors be calibrated experimentally.

A large number of experimental studies have been published on cascade impactor design and performance in the laboratory environment. Most of these have been reviewed in the dissertations of Marple[8] and Rao.[9] Recently, Cushing, et al[10] have presented calibration data on several commercially available cascade impactors. Figure 8 shows a schematic of the University of Washington Mark III impactor. The design of the Mark V is similar to that of the Mark III.

During the test program, University of Washington Mark V impactors were used. Sampling procedures as outlined by Harris[11] were followed.

Collection Substrate Materials--

Most impactors have collection stages which are too heavy for obtaining accurate measurements of the mass of the particles collected in each size fraction. Weighing accuracy can be improved by covering the stage with a lightweight collection substrate made of aluminum foil, teflon, glass fiber filter material, or other suitable materials, depending upon the particular application. Some manufacturers now furnish lightweight inserts to be placed over the collection stages. With such arrangements, it is possible to make accurate determinations of the masses collected on various stages without risking reentrainment due to overloading.

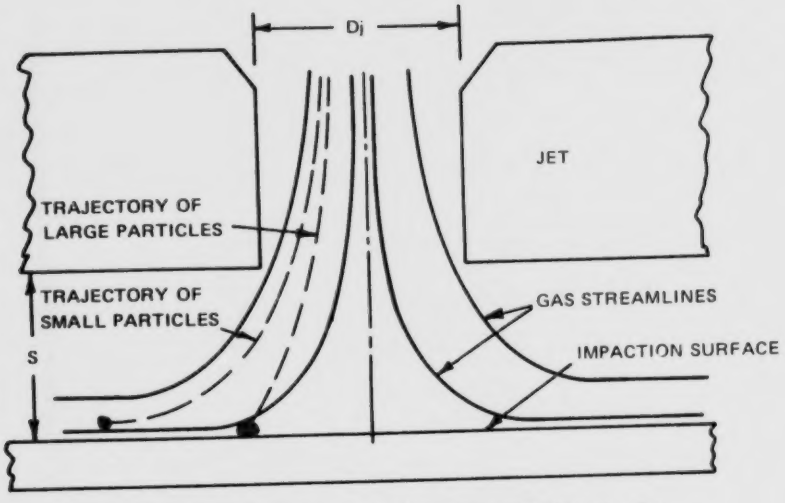

A. TYPICAL IMPACTOR JET AND COLLECTION PLATE

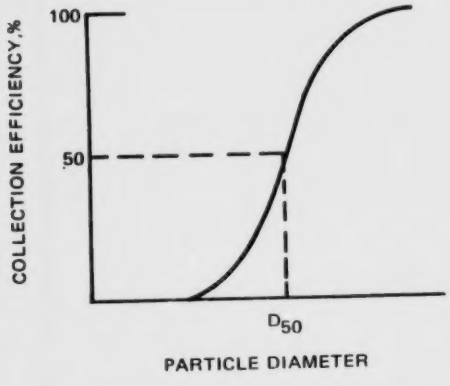

B. GENERALIZED STAGE COLLECTION EFFICIENCY CURVE

4266-67

Figure 7. Operation principle and typical performance for a cascade impactor.

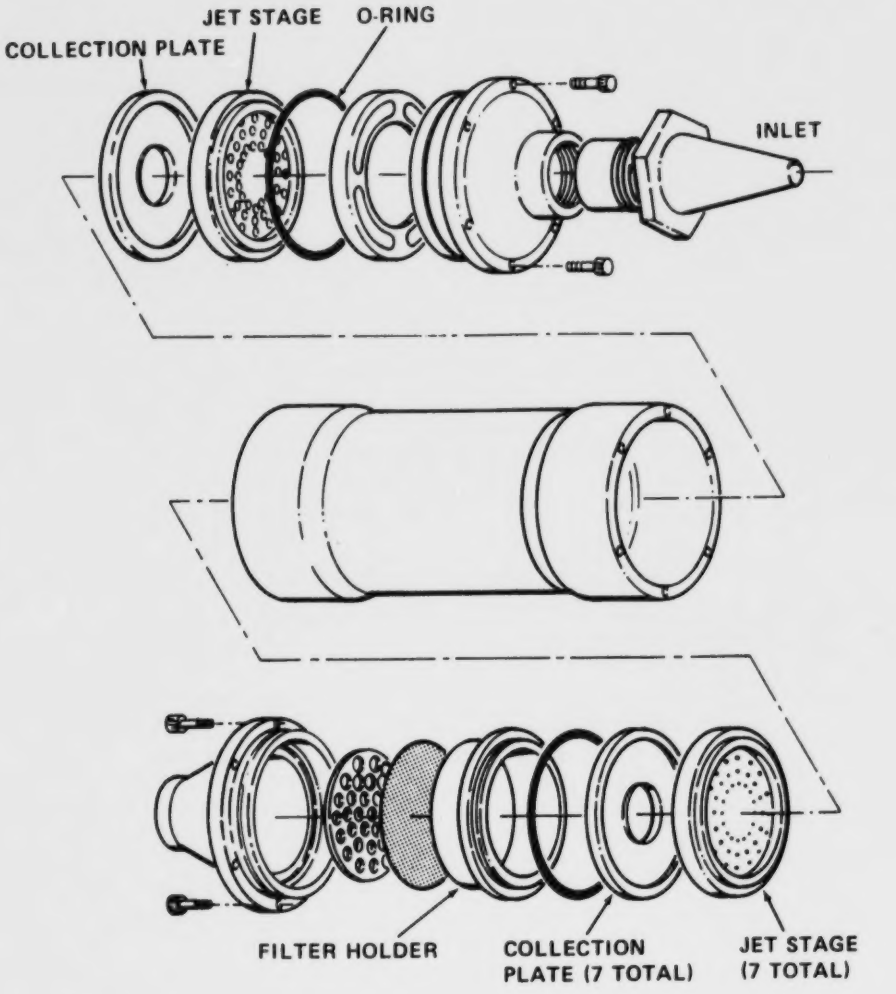

Figure 8. University of Washington Mark III Source Test Cascade Impactor.

The use of greased aluminum foils, Mylar, or lightweight glass fiber filter mats as collection substrates tends to alleviate the problem of weighing accuracy, but new problems due to substrate weight changes are introduced. Although normal substrate preparation includes baking and desiccation before the initial weighing, it is frequently found that weight losses can occur when sampling clean air. SoRI has conducted tests for the EPA to investigate this phenomenon in detail (Felix, et al[12]). It was found that with careful handling weight losses for glass fiber substrates could be kept below 0.2 mg. This loss is attributed to loss of fibers which stick to seals within the impactor and to "superdrying" when sampling hot, dry air. Weight losses of 0.2 mg are small compared to normal stage catches when sampling particles, and thus are generally within a tolerable range for sampling errors.

When sampling clean, hot air with greased substrates, more severe weight losses can occur. Some of the weight lost on upper impactor stages reappears as weight gained on the backup filters. This is interpreted as an indication that grease may flow or be blown off the collection surfaces.

In some cases (e.g., paper mill recovery boilers and oil fired power plants), the particles are adhesive and bare metal or other surfaces can be used to obtain reliable data.

Glass fiber substrates weight gains have been a source of very large errors when sampling industrial flue gases. Under EPA Contract 68-02-2131 SoRI has performed extensive studies (Felix, et al[12]) to determine the magnitude of weight gains, their cause, and to recommend solutions. These tests were initiated after it was discovered that glass fiber substrates gained as much as 4-5 mg when sampling filtered gas.

At the same time, a laboratory study of greases for use on collection plates was also conducted. Tests were performed to ascertain which of the available greases and glass fiber filter media are most suitable for flue gas sampling. Greases are probably not useful for temperatures above 177°C (350°F). For higher temperatures glass fiber filter material can be used. Of nineteen greases tested by heating in the laboratory and exposure to flue gas in the field, only Apiezon H grease was found to perform satisfactorily at temperatures above 149°C (300°F).

In experiments designed to evaluate the use of filter materials as impactor substrates it was found that mass increases occurred as a result of exposure to flue gas for all of the fiber media tested. Laboratory and field studies were conducted which were directed toward development of a method by which glass fiber filter material can be passivated to SO_x induced mass gains. These studies indicate that a H_2SO_4 wash followed by a thorough distilled water and isopropanol rinse, drying, and baking,

augmented by in situ conditioning, offers the best hope for reduction of $\overline{SO_x}$ induced mass gains. Reeve Angel 934AH glass fiber filter material performed best among the media tested.

Ultrafine Particle Sizing Techniques

There are two physical properties of ultrafine particles (diameter <0.3 μm) which are size dependent and which can be predicted with sufficient accuracy under controlled conditions to be used to measure particle size. These are the particle diffusivity and electrical mobility. Although ultrafine particle-size distribution measurements are still in a developmental stage, instruments are available which can be used for this purpose, and a number of field measurements have been made.

Size Selective Removal of Ultrafine Particles--

Sizing information for ultrafine particles is obtained by using a size discriminating physical property, such as diffusional mobility or electrical mobility, in a controlled configuration to enable one to effectively form a size selective filter. These pseudo filters are somewhat analogous to low frequency bandpass filters used in electronics. When used in conjunction with a cumulative concentration indicator (counter), these filters can be used to obtain concentration versus size information. By placing a filter upstream of the counter, a decrease in signal occurs. This decrease in signal indicates the total number of particles which were removed by the addition of the pseudo filter.

The D_{50} of a filter is defined to be that size for which fifty percent of the particles are passed by the filter and fifty percent of the particles are captured. If the penetration curve for the filter is sufficiently sharp, one can consider that all particles smaller than the D_{50} for this configuration are captured and all particles larger than the D_{50} are passed through the filter, thus one can pick a series of pseudo filters which will divide the ultrafine size range (0.01 μm to 0.3 μm) into several size windows.

Using a counter one can measure the total number of particles that penetrate a given filter (D_{50_1} <d). The signal is then attenuated by inserting a different filter which effectively removes all particles smaller than its own D_{50} (D_{50_1} <D_{50_2}). The window concentration, as determined by the decrease in signal, is assigned to the geometric mean diameter of the size window (D_{50_1}, D_{50_2}). By sequentially inserting additional filters having larger D_{50}'s and measuring the corresponding signal decrease, one can obtain concentration versus size information over the ultrafine size range.

Electrical Mobility Measurement Techniques--

The most complete set of experiments performed in order to determine the relationship between particle size and charge were reported by Hewitt.[13] These experiments confirmed theoretical predictions that there exists a unique charging rate for each particle size if the charging region is homogeneous with respect to space charge density and electric field.

In the course of this work, Hewitt developed a mobility analyzer. In Hewitt's experimental work, the particle size was known, and the mobility was used to determine charge. If, however, the particle charge were known, the mobility could be used to determine the particle size. This concept has been used by Liu, Whitby, and Pui[14] at the University of Minnesota to develop a series of Electrical Aerosol Size Analyzers (EASA). A ruggedized field unit based on the earlier Univeristy of Minnesota designs is now commercially available (Thermo-Systems, Inc., 2500 North Cleveland Ave., St. Paul, Minnesota 55113) and has been successfully used for field testing (Liu and Pui[15] and Sem[16]). Variation in the strength of the electric field applied to the center collection rod is used to form different size selective filter configurations. As the strength of the field is increased, progressively larger particles are stripped away.

Optical Measurement Techniques

Real time concentration information in the 0.3 μm to 2.0 μm size range can be obtained by using commercially available optical particle counters in conjunction with the Sample Extraction Dilution System described below. This real time analog data allows one to observe emission fluctuations as well as obtain an integrated time average.

In the optical paricle counter individual particles pass through a small viewing volume where they scatter a light beam. This scattered light is detected by a photodetector. The amplitude of the scattered pulse determines the size of the particle and the presence of a pulse indicates the presence of a particle. Pulse height analysis is then performed on the signal for the optical particle counter to obtain the desired sizing information.

Sample Extraction-Dilution System

When possible, in situ sampling is preferred because it eliminates many condensation and sample loss problems which occur with extractive sampling. Unfortunately, the existing ultrafine sizing techniques do not lend themselves to instack sampling. Particulate concentrations are extremely high in an industrial flue and vary by orders of magnitude from one industrial process to another and from the inlet side of a control device to the outlet of the same device. Temperature, pressure, moisture

content, and the physical properties of the particles also vary widely from one industrial process to another. Because of this complexity and the limited useful concentration range for these sizing techniques extensive sample dilution and conditioning is required to obtain information on ultrafine particles in an industrial gas stream.

Figure 9 is a block diagram of the sample extraction-dilution system developed for this purpose by Southern Research Institute. A 15 liter/min sample flow is removed from the process stream through a rigid heated probe, a flexible heated hose, and a cyclone, into a "T" where the flow splits. The excess flow is dumped to ambient and the desired sample flow (0.05 to 15 alpm) goes into the diluter via a calibrated orifice and an optional diffusional type absorber bank. The cyclone, orifice, and absorber bank are housed in a heated conditioning chamber so that all components of the system except the diluter can be maintained at 400°F to prevent condensation. Pressure taps for the cyclone and the orifice allow continuous monitoring of the cyclone flow rate and the sample flow rate for the diluter by reading the pressure drop across the respective component. The sample gas enters the dilution chamber at the apex of a perforated cone into which clean, dry air is pumped through the perforations, creating a highly turbulent mixing zone. Figure 10 shows the calibration data reported by Ragland[17] for the SoRI Diluter shown in Figure 11. At a downstream point from the diluter cone, after adequate mixing has occurred, the diluted sample is extracted and conveyed to the sizing instrument. This diluted sample passes through a diffusional dryer where any remaining moisture is removed (the major drying action is accomplished by using dilution air which has been passed through an ice bath condenser and silica gel column). The instrument exhaust lines are returned to the diluter to maintain a minimal pressure drop across the instruments. Further drying of this recycled air is accomplished by passing this instrument exhaust gas through an absorption drier.

Changing the sample air flow and the dilution air flow allows one to change the dilution ratio (the ratio of the total flow to the sample flow). As shown in Figure 9, sample air and dilution air flow rates are controlled by two bleed valves on the dilution air pump, one upstream of the pump (#1) and one downstream (#2). Manipulation of these valves changes the internal pressure of the diluter which, in turn, sets the sampling rate. As the pressure in the diluter is reduced, the sample flow rate is increased. In practice, the operation of these valves changes the dilution air flow only slightly (approximately 10%) for a many fold change in sample flow. Gross changes in sample flow are accomplished by changing orifice meters.

Because the Electrical Aerosol Analyzer (EAA) operation depends upon placing a known electrical charge on the aerosol particles, the particles must be in a state of charge equilibrium

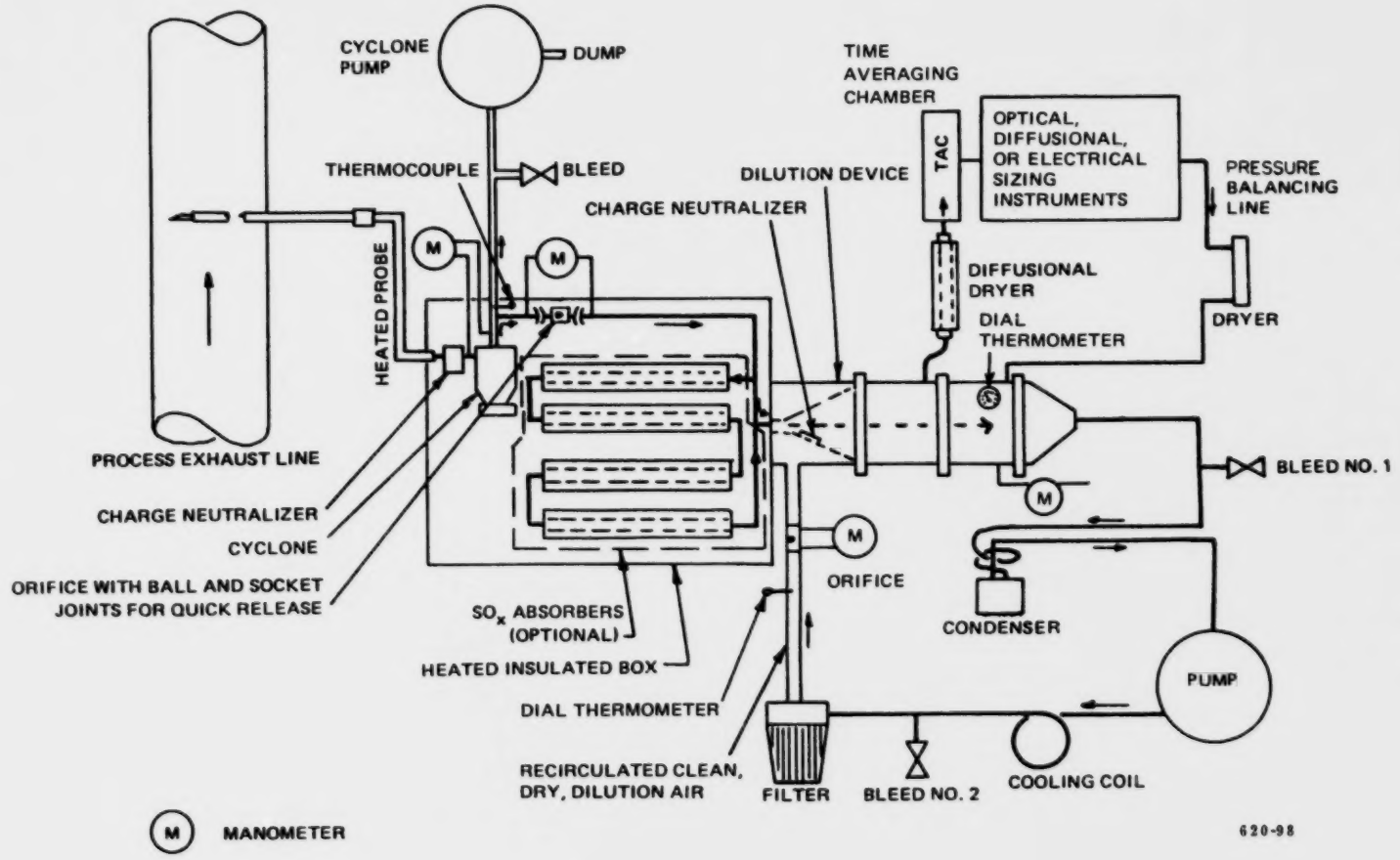

Figure 9. Modified Southern Research Institute SEDS.

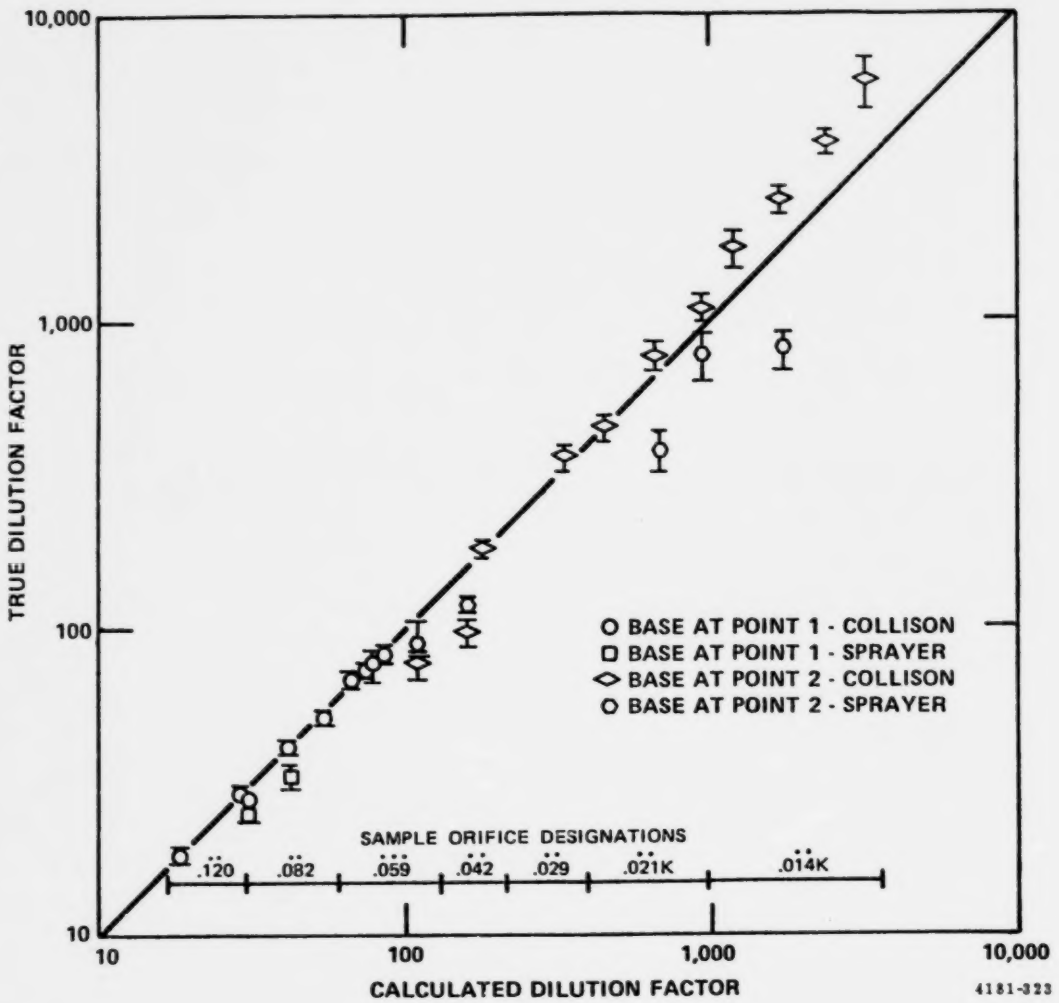

Figure 10. Theoretical dilution versus actual dilution for 0.15 μm particles in the SoRI diluter.

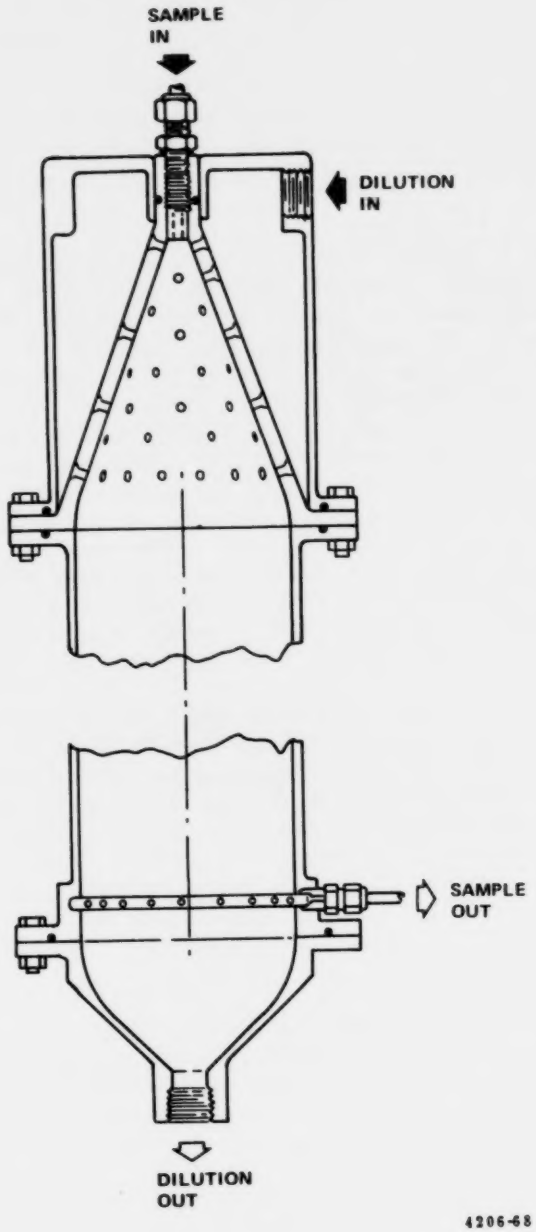

Figure 11. SoRI diluter, cut-away view.

with zero net charge upon entering the EAA. To accomplish this needed neutralization, two 500 μc Polonium-210 strips are mounted in the cone of the diluter as shown in Figure 9.

Data Reduction Techniques

The particle sizes reported here are based on the assumption that the particles are homogeneous spheres. The density of the particles plays no role in the EAA performance although it is required for conversion of the measured volume distribution to a mass distribution.

The cascade impactor data were reduced using a computerized Cascade Impactor Data Reduction System (CIDRS) developed by Southern Research Institute. The program is described in EPA report 600/7-78-132a (44 pages) and described in extensive detail in EPA report 600/7-78-042 (591 pages), and updated in EPA report 600/9-80-004 (pp. 146-66). Input to the program includes the impactor geometry used, individual stage calibration constants, catch weights, gas composition, temperatures, pressures, flow rates and other pertinent sampling information from which the particle separation diameters, D_{50}'s, and particulate loadings by particle size are calculated. An osculating polynomial technique is used to permit extrapolation of the size distribution beyond the D_{50} of the first stage. This polynomial is forced to zero slope in the cumulative size distribution at the maximum particle size found in the sample from each run.

The fitted distributions from several runs made under similar test conditions were averaged and are presented in a variety of forms to suit the particular uses for which the data may be intended. Confidence intervals based on the scatter in the data are included in most figures of averaged results from the impactors. Ninety percent (90%) confidence intervals are used throughout this report. These confidence intervals reflect only the observed scatter in the data and do not include calibration uncertainties. The latter are generally small as compared to the former.

Electrical mobility data were reduced using a computerized Simplex technique to compensate for the cross channel sensitivities of the Model 3030 EASA. The data obtained with the EASA in the sizes 0.013 μm, 0.42 μm, 0.75 μm, and in some cases 0.024 μm of questionable validity because the concentrations present were below the noise levels for the instrument. For this reason the data for those sizes were not included in this report. The equations involved in EASA data reduction are those reported by Cushing and Smith.[18] The Simplex programming techniques have been described by Liu and Kapadia.[19]

SECTION 5

MECHANICAL DEVICES

DEEP BED FILTER

The first device to be fabricated and tested was the deep bed filter shown schematically in Figure 12. The dimensions of this device are based on a theoretical study which predicts 82% collection of diesel exhaust particles when used with a 10 cm thick fiber mat of 10 μm fiber diameter and a porosity of 0.99.[5] This device has a very large face area due to the downward gas flow. This geometry results in a greatly reduced flow velocity through the filter mat which enhances particle capture by the filter fibers and reduces reentrainment. In addition, should the filter be subject to blinding, the large face area should increase the lifetime of the device. The geometry would also be convenient for use with interchangeable filter elements.

The filter box was fabricated at SoRI for use in a joint testing program with the Automotive Research Laboratory of the DOT Transportation Systems Center in Cambridge, Massachusetts. Screening tests were conducted at SoRI to determine suitable filter materials. The materials tested were air conditioning filters, chopped fiber insulation of the type normally blown into attics of houses, fiberglass batts derived from roll insulation, and long fiber spun glass (angel hair).

Test results showed that 10 cm of air conditioning filters had little or no collection efficiency for diesel particulate matter. Ten cm of chopped fiber insulation did better, with a 39% collection efficiency. Both the fiberglass batts and the spun glass demonstrated efficiencies in the 80-90% range. Consequently, these two materials were chosen for the DOT test. The fiberglass batts had a fiber diameter of about 15 μm and, for the sample tested, a porosity on the order of 99%. However, since the material was very compressible, the porosity was highly variable. The angel hair had a 20 μm fiber diameter and an undefinable porosity since it came compressed into 0.45 kg (1 lb) bags and could easily be pulled apart with the fingers.

Test Results

The test program at DOT utilized the GM 5.7 liter diesel engine installed in a test cell at the DOT facility in Cambridge.

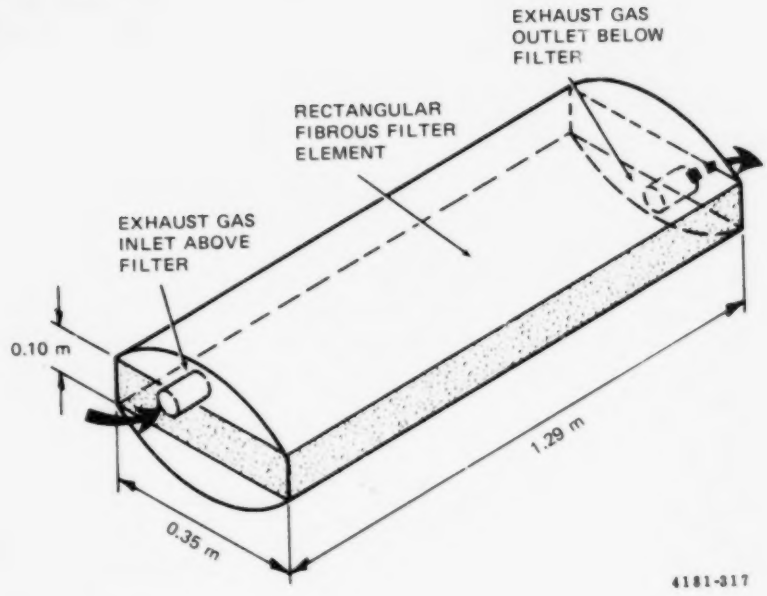

Figure 12. Deep bed filter.

Tests were run at engine speeds equivalent to 48 and 88 km/hr (30 and 55 mph) which produced gas velocities of 0.17 and 0.27 m/sec through the filter. During two of the tests, the exhaust temperature was lowered by wrapping water cooling lines around the exhaust pipe. This resulted in a temperature drop at the control device of about 15°C. During other tests, the exhaust temperature at the device was raised by wrapping fiberglass insulation around the exhaust pipe. This resulted in a temperature rise of about 20°C. The effects of this were evidenced by slight increases in particle concentration occurring at reduced temperatures and slight decreases for elevated temperatures. The pressure drop across the control device was monitored and the testing was discontinued if the pressure became too high or rose quickly and then leveled out or dropped, an indication that the gas was finding an alternate path through or around the filter material.

Initially, the deep bed filter demonstrated about 90% collection efficiency at 88 km/hr (55 mph) and 95% efficiency at 48 km/hr (30 mph) using 15 cm of fiberglass batts for the filter material. These values were degraded, however, as the pressure drop across the filter rose and gas sneakage was induced. On site equipment modifications reduced the amount of sneakage present but were incapable of completely eliminating it. Figure 13 shows the pressure drop across the filter for one of the tests. In this example the pressure curve starts at a low value, rises quickly as the cake builds up and then levels off. This type of pressure behavior proved to be typical for every run in the test series (12 tests). Figure 14 shows a set of fiberglass batts that were used in one of the tests. The front surface, which cannot be seen in this figure, is very black and shows signs of building a cake of particles. The edges are also very black, which implies the presence of gas sneakage, an effect that would explain the leveling out of the pressure curve of Figure 13. Collection efficiencies measured after the pressure drop curve had leveled off were quite low. In one example the efficiency measured as low as 6% although values of about 40% at the termination of testing were more typical. However, the final efficiency value may be a function of how long the filter was allowed to run after the onset of sneakage. Figure 15 compares the size dependent collection efficiencies before and after the onset of sneakage for the same test (11/14/79) referred to by Figure 13.

The behavior of the spun glass in the deep bed filter was very similar to that of the fiberglass batts. Initial efficiencies using about 15 cm of the material were in the 80-90% range for the 88 km/hr equivalent engine speed. This material appeared to be less susceptible to sneakage than the fiberglass batts. This is probably due to the less rigid form of the spun glass which should allow the material to flow to fit the container. Two runs were made with this material. In the first test, the pressure curve started to break over, an indication of the onset of sneakage.

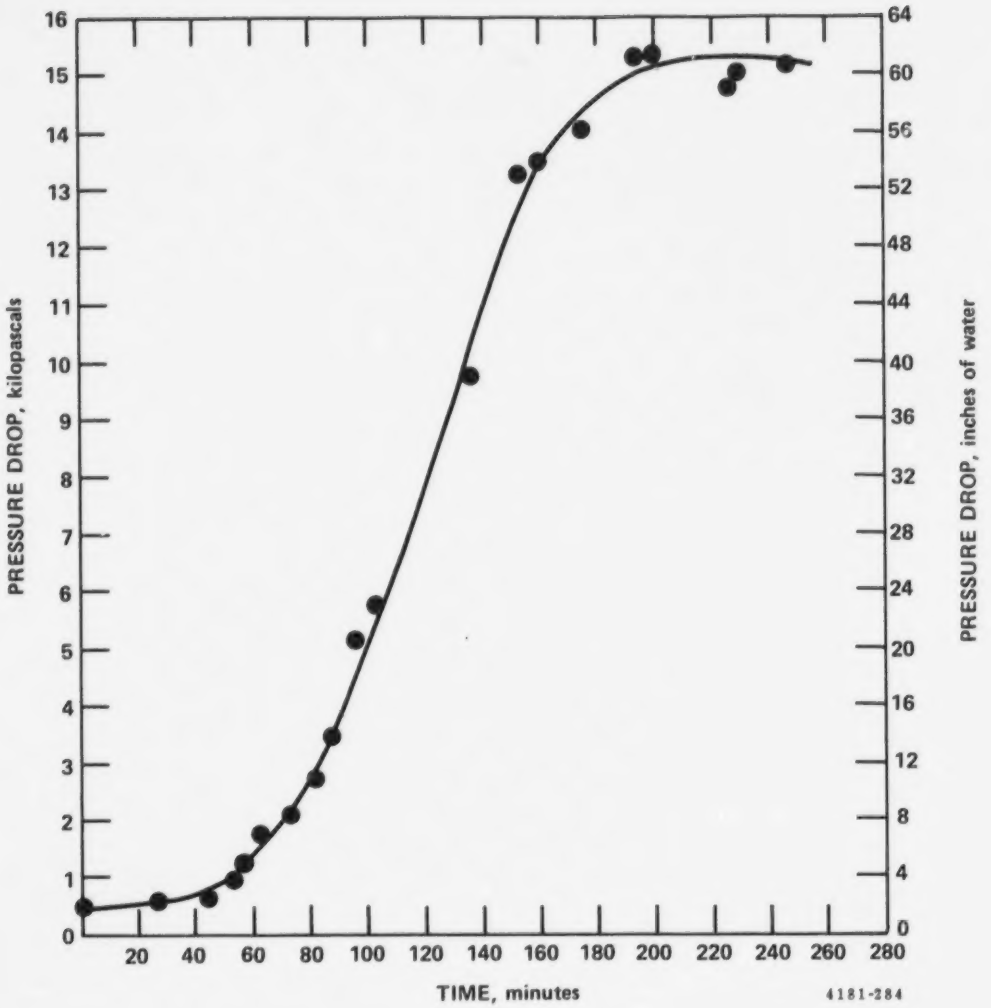

Figure 13. Pressure drop across fiber glass batt (11/14/79).

4181-824

Figure 14. Fiberglass batts with accumulated soot.

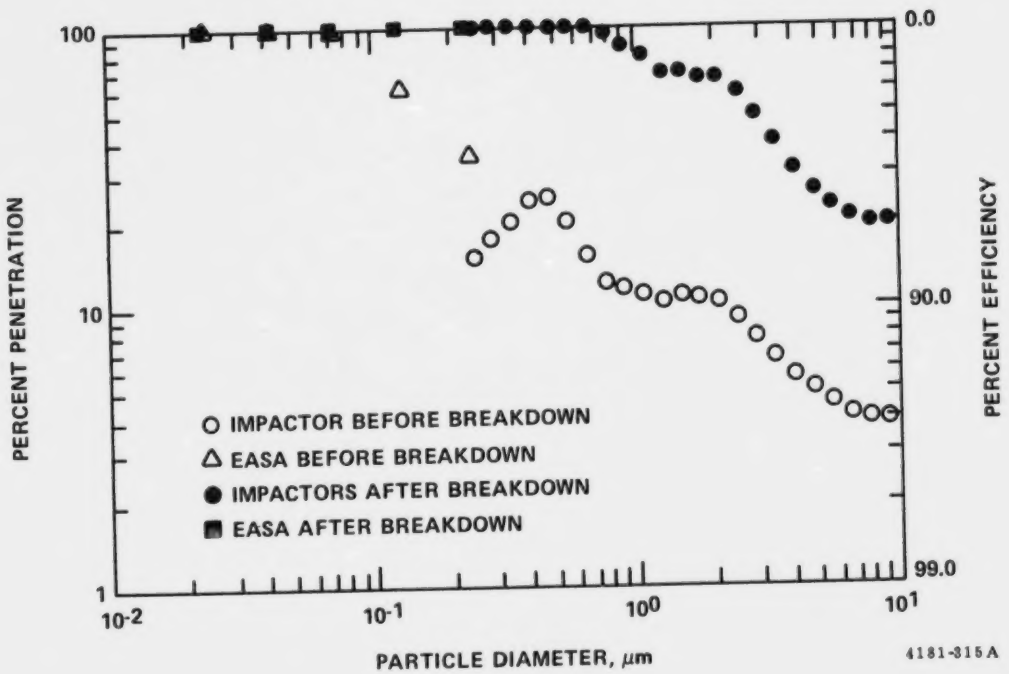

Figure 15. Efficiencies before and after onset of sneakage for deep bed filter using fiberglass batts (11/14/79).

This curve is shown in Figure 16. Figure 17 shows the second run with spun glass, in which no break in pressure rise was evident. This run was terminated due to high back pressure (23 kPa or 92 in. H_2O). The efficiencies were essentially the same for both runs as the measurements were made before the onset of sneakage in the first run.

During a second series of tests at DOT, the deep bed filter was run using a stainless steel fiber mat which had been fabricated in Belgium for this test series. This material was composed of 12 μm stainless steel fibers which were spun into a 0.64 cm (0.25 inch) thick mat which was then fused on both sides to give it some rigidity. The calculation called for a 10 cm thick bed but only 2.5 cm (four layers) were used in these tests. The first test was run at 88 km/hr (55 mph) equivalent speed in an upward gas flow configuration to determine whether the soot could be dislodged from the face of the filter mat by rapping the filter box. However, the test was cut short when the backpressure rose from 0.9 to 1.4 kPa (3.6 to 5.6 in. H_2O) in 25 minutes and then leveled out for the duration of the one hour test. After the test, the filter box was opened and the filter material was examined. There was obvious soot trails on the sides of the fiber bed indicating severe sneakage. There was no evidence of soot between the layers. The soot cake on the first surface of the fiber mat was very dense and tenacious. It could not be shaken off of the surface. Attempts to remove the cake by using a backflow of compressed air were only slightly successful but the compressed air permanently compressed the filter material. Successful cake removal could only be achieved by scraping the face of the filter. The cake appeared denser here than it did with the fiberglass batts used in the November test but this was probably due to the smooth surface of the stainless steel. A retest of this device using a downflow configuration resulted in mechanical failure when the pressure on the filter collapsed the support screen in the filter box.

The question of whether the particles will ever work their way into and through the filter mat or just pile up on the surface remained unanswered. If the particles will work through the mat, it may be possible to use the mat as an agglomerator followed by a collection method suitable for larger particles such as a cyclone. Following the DOT test series, an answer was sought at the SoRI facility in Birmingham. After the bottom screen was rigidly attached to the filter box, one sheet of the stainless steel fiber mat was placed in the box and sealed in with RTV silicon. No metal screen was placed on top of the mat. The device was run for about 2 hours at 88 km/hr. During this time the pressure had climbed to 5.8 kPa (23 in. H_2O) but had dropped sharply several times in the process. This normally indicates the formation of some low pressure pathway around or through the device. Collection efficiency was 28% for this run. When the device was opened, it was observed that several holes had been formed in the mat. Further examination showed that

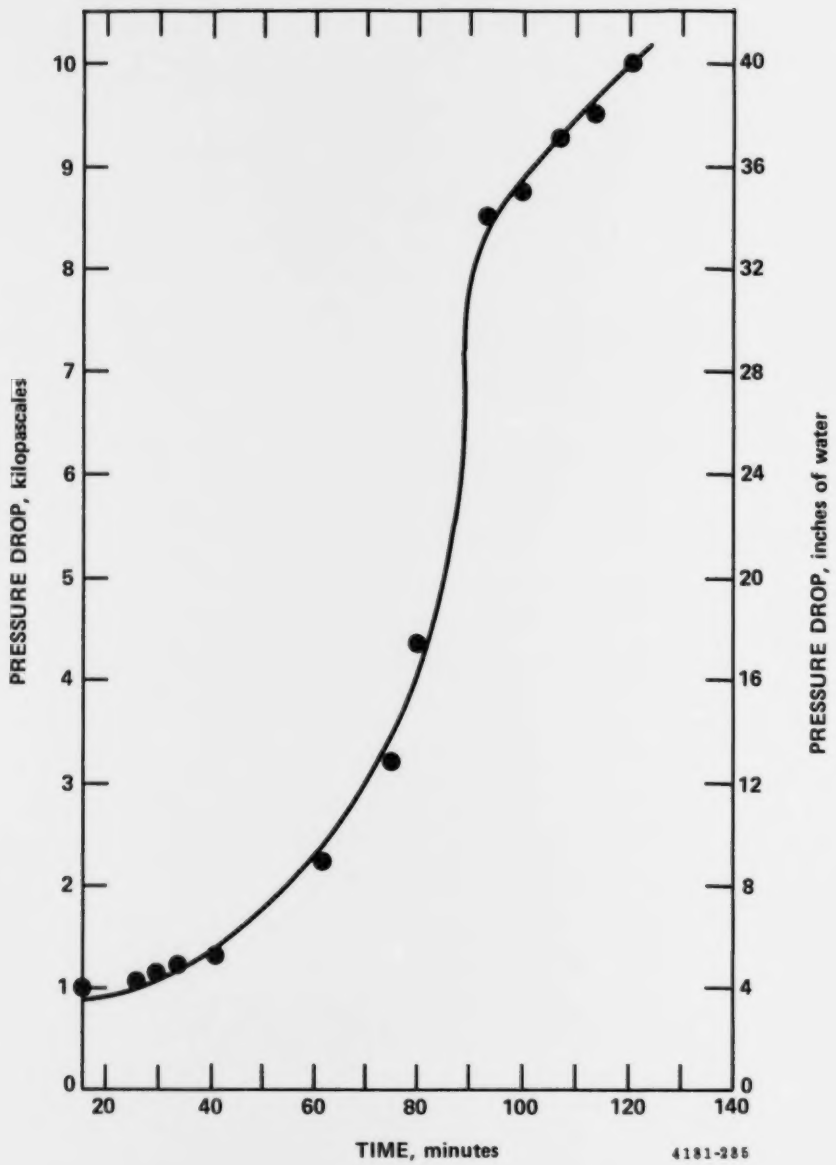

Figure 16. Pressure drop across glass wool (11/12/79).

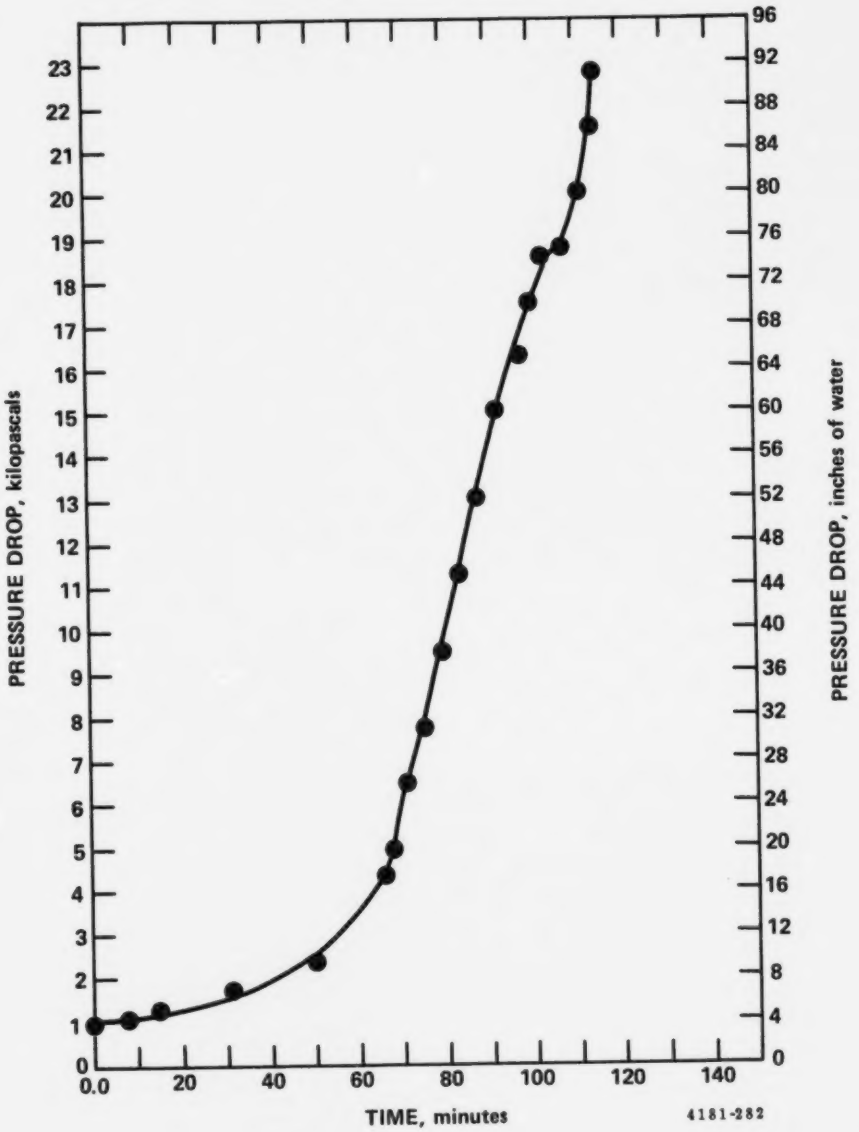

Figure 17. Pressure drop across glass wool (11/13/79).

the filter material near the inlet had been effectively destroyed. The sintered outer surfaces were very brittle; the inner fibers were either gone or so thoroughly heated that they crumbled to a powder at a touch. Figure 18 shows the damaged area. The mat was cut further down and split to see if the particles were working through. The fibers were lightly discolored near the back and became darker closer to the front. A cake was beginning to form on the front surface. The only places where the mat was black all the way through were around the damaged area, and the fibers had begun to get brittle. The damaged region occurred about where the downwardly deflected exhaust stream would hit the mat.

The expanded metal top screen which was used on previous runs had not been in place on this test. It is not known whether the addition of the screen would have served to equalize the heat of the exhaust stream and possible prevent the burning out of the fiber mat. Although this test did not answer the question of whether the surface cake prevents mat penetration, the test was not rerun as there were other devices waiting to be tested. However, later information obtained using the gravel bed filter indicated that the cake would have blinded the filter before a significant amount of particulate matter filtered through the mat.

Table 1 and Figures 19-24 summarize the results of the deep bed filter testing program. The 900 rpm engine speed corresponds to a 48 km/hr (30 mph) vehicle speed and 1700 rpm corresponds to 88 km/hr (55 mph). The variations between the collection efficiencies reported by the different sampling devices for a given test are largely due to different sampling times during the rapidly changing life cycle of this control device. Other contributing factors are different principles of measurement, different temperatures at which the measurements were made, and different size ranges detected by the instruments.

Conclusions

The use of a fine fiber filter to capture diesel particles does not appear to be practical due to the tendency toward formation of a cake on the face of the filter. This cake of collected soot reduces the gas flow through the filter which results in an increase in the pressure drop across the device. The pressure continues to increase until either it impedes the operation of the engine or a lower pressure route around the filter mat is established. Once a route for gas sneakage is established, the collection efficiency of the device drops sharply.

GRAVEL BED FILTER

The next type of device examined was a gravel bed filter. The concept calls for agglomerating the particulate matter so that it can be collected in a large particle separator such as a cyclone.

Figure 18. Damaged area on stainless steel filter (5/22/80).

TABLE 1. SUMMARY OF DEEP BED FILTER TESTS

Test Location & Date	Engine Speed & Exhaust Temperature at Device	Filter Material	% Efficiency					NOTES
			Dilution Tunnel	Mass Filter	Cascade Impactos	Optical Counter	EASA	
DOT 11/14/79	1700 rpm 225°C	15 cm Batt Fiberglass	85	-	89	55	49	Increasing pressure drop leveled off at 15 kPa after 3 hours. Inspection showed ruptured filter material. Upper efficiencies are before breakdown; lower numbers after. Ref. Figures 13 and 15.
			58	45	6	0	0	
DOT 11/15/79	1700 rpm 227°C	New 15 cm Batt Fiberglass	-	88	-	-	-	Gas flow configuration changed from downdraft to updraft. Test terminated due to sudden severe pressure increase. Inspection showed filter material had moved upward & blocked exit port. Ref. Figure 19.
DOT 11/15/79	1700 rpm 236°C	Same Batt	-	72	-	98	92	Resumption of same test. Pressure drop leveled off after 1 hour. Total test time 5.75 hours. Inspection showed ruptured filter material. Rupture presumably occurred when pressure leveled off. Efficiencies shown are before and after the pressure curve leveled off. Ref. Figure 19.
			59	-	58	78	0	
DOT 11/12/79	1700 rpm 222°C	15 cm Glass Wool	74	77	69	95	72	Sneakage seems to be less of a problem than with fiberglass batts. Pressure drop increased from 0.75 kPa to 10 kPa over 2 hour test. Ref. Figure 16.
DOT 11/13/79	1700 rpm 238°C	15 cm New Glass Wool	83	-	92	-	-	Terminated at 1.75 hours due to rise in pressure drop (1 kPa to 23 kPa). Ref. Figures 17 and 20.
DOT 5/7/80	1700 rpm	2.5 cm SS Mat.	-	54	18	-	-	Sneakage built up. Upflow configuration. Ref. Figure 21.
DOT 5/8/80	1700 rpm	2.5 cm New SS Mat.	68	70	72	-	39	Downflow configuration. Pressure collapsed filter support to allow sneakage during test. Upper numbers are before failure; lower numbers after. Ref. Figures 22 and 23.
			30	30	-	-	0	
SoRI 5/22/80	88 km/hr 157°C	0.6 cm New SS Mat.	-	28	-	-	-	Holes formed in mat due to localized excess heating. Ref. Figure 24.

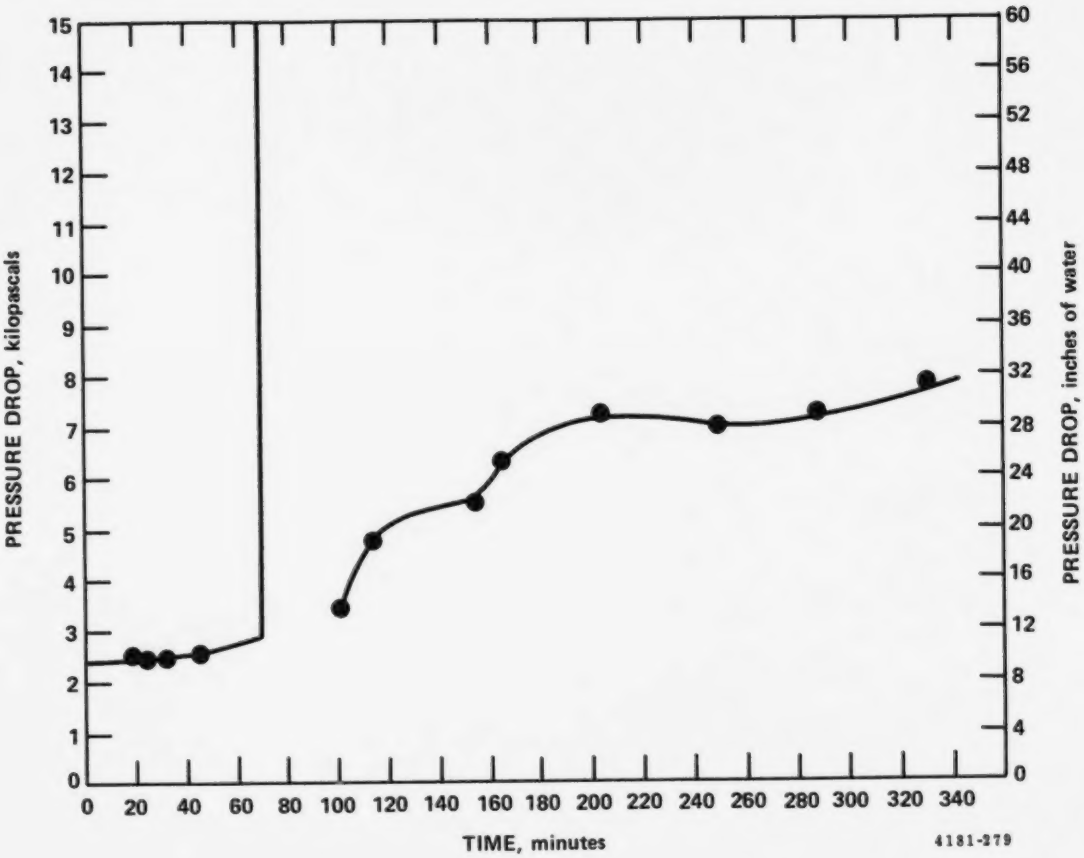

Figure 19. Pressure drop across fiberglass batt (11/15/79).

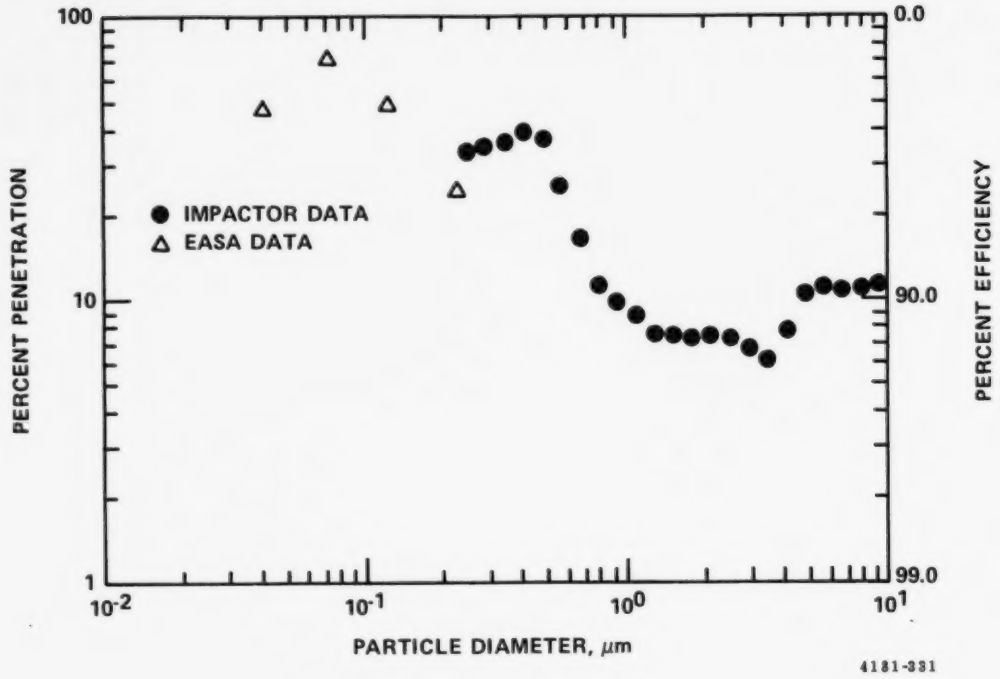

Figure 20. Efficiency for deep bed filter using 15 cm of glass wool (11/12/79).

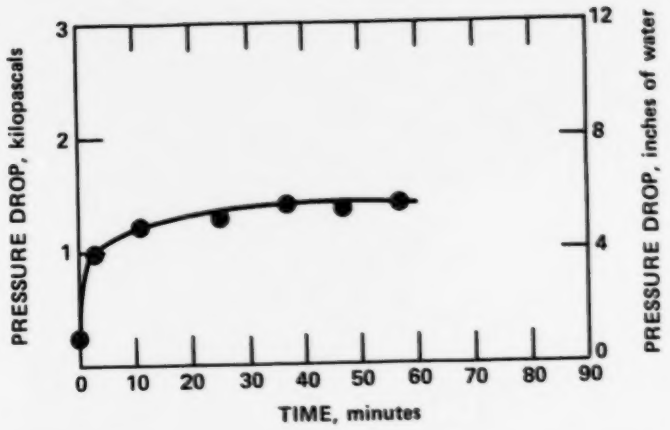

Figure 21. Pressure drop across deep bed filter with steel fiber mat (5/7/80).

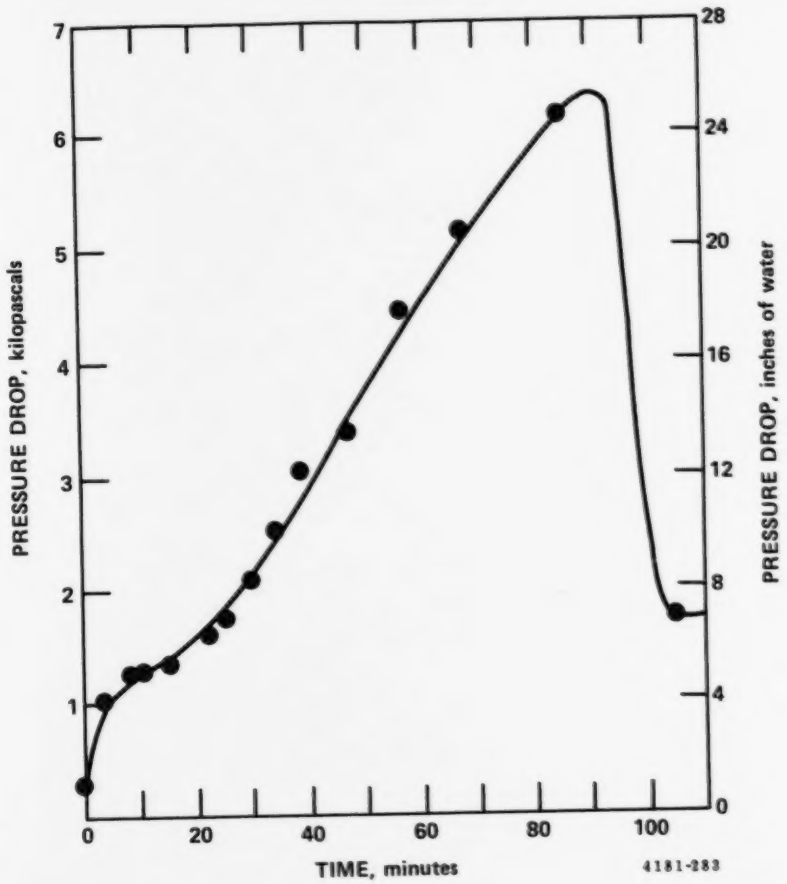

Figure 22. Pressure drop across deep bed filter with steel fiber mat (5/8/80).

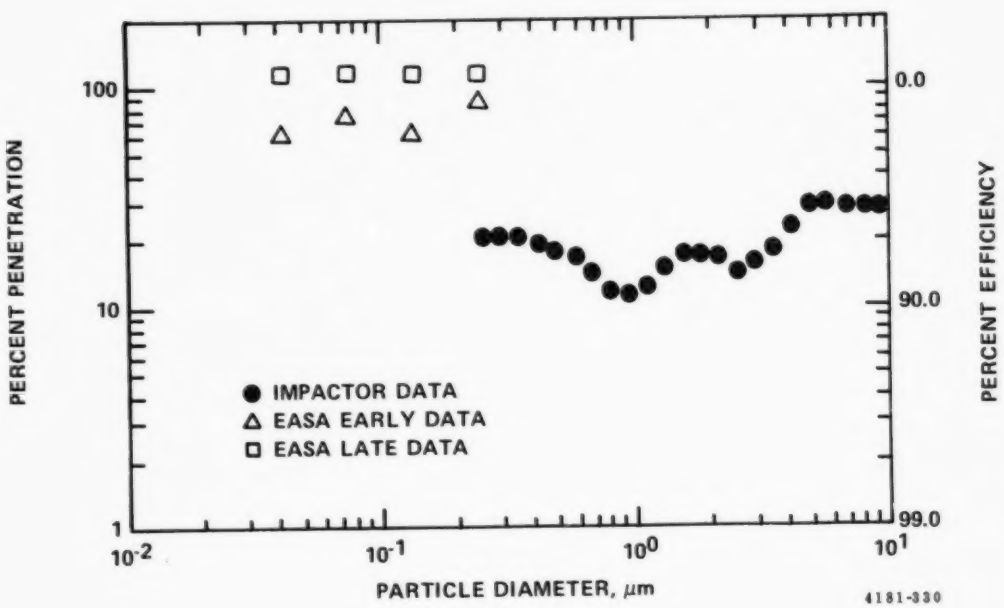

Figure 23. Efficiency for deep bed filter using stainless steel filter mat (5/8/80).

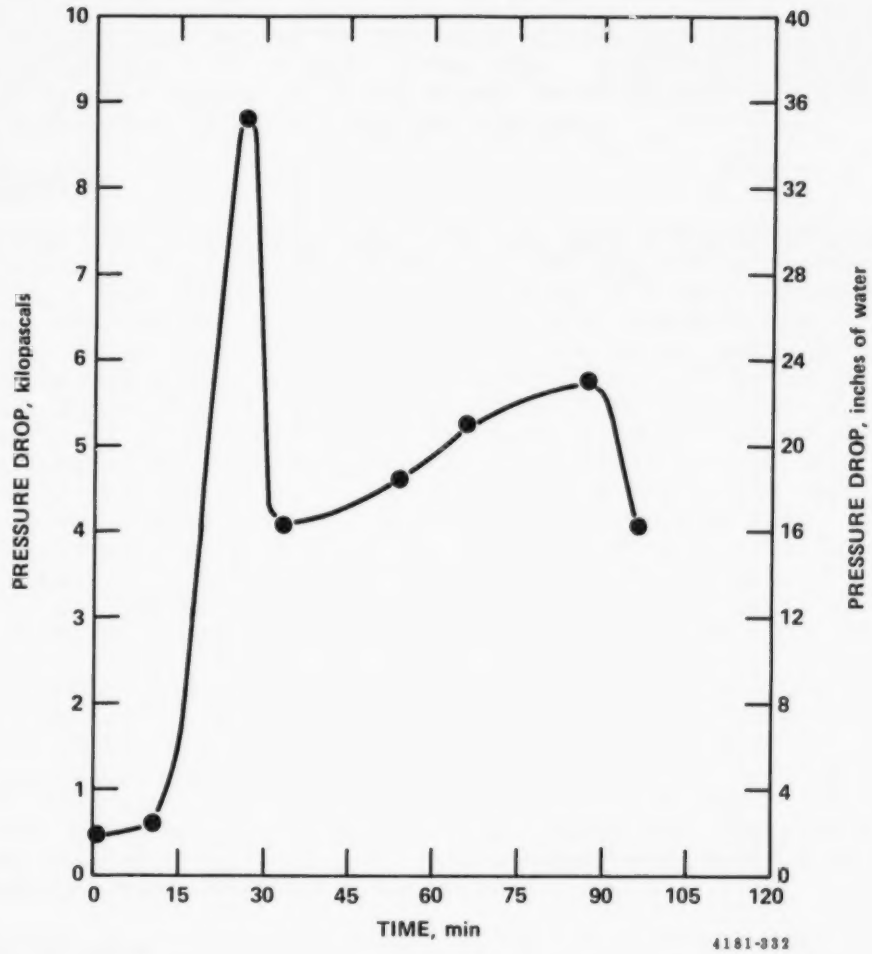

Figure 24. Pressure drop across steel fiber mat (5/22/80).

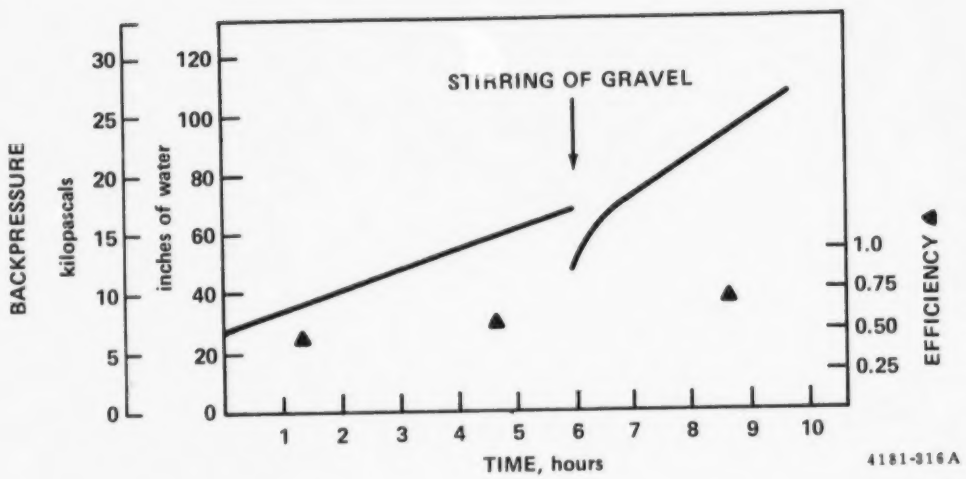

Figure 25. Gravel bed filter efficiency and backpressure.

piling up on the top surface. This surface deposit was easily broken up when the bed was smoothed out and releveled. This mild stirring of the shot gave rise to the break in the ΔP curve shown in Figure 25. However, the pressure quickly resumed its upward trend and reached 27 kPa (108 in. H_2O) after 10 hours of operation. Inspection showed that a thick surface layer of soot had again accumulated. The collection efficiency measured at the end of the test was 72%.

At this point the system was modified to remove the screen on top of the bed, install a baffle so the gas stream would not dig holes, and install a rake so the top 3 cm of the shot could be stirred to break up the top layer. Figure 26 shows the back pressure as a function of time during the tests with stirring. A distinct reduction in pressure drop occurs each time the bed is stirred. There is a downward trend which turns up again, perhaps due to filling of lower levels. There was also a large black puff of soot occurring at the end of the exhaust pipe each time. Optical particle counter data were taken during these tests. The results of the 30 minute stirring test are shown in Figure 27. These peak numbers are ballpark numbers only since the Climet particle counter's dead time was up to 80% during the puff. Experiments have shown that when this happens, the instrument's size response becomes nonlinear with large particles being emphasized. Collection efficiencies averaged 40% for these tests. The performance during the one hour stirring interval tests was essentially the same, with collection efficiencies down to 33%.

Table 2 summarizes the results of the gravel bed filter test program. The efficiencies listed are derived from mass filter data. Limited size dependent data were taken using the Climet optical particle counter. It is not apparent from these data that any agglomeration effects are occurring. Therefore the gravel bed filter must be treated as a particle collector and not as a particle agglomerator.

Conclusions

The granular bed filter is a concept which may prove applicable to the diesel exhaust problem. Although the collection efficiency was not as high as that of a fiber filter, the gravel bed has the important advantage of being cleanable, whether by mechanical or chemical means.

CONDENSATION TRAPS

A condensation trap named the Aut-Ainer is being developed specifically as a diesel exhaust control device by Eikosha Co. in Japan. Figure 28 shows a conceptual sketch of two Aut-Ainers in which there are three bands of stainless steel mesh followed by a cyclone for soot collection. This mesh is a coarsely woven belt of 0.2 x 0.4 mm flat wire which has been rolled around the central

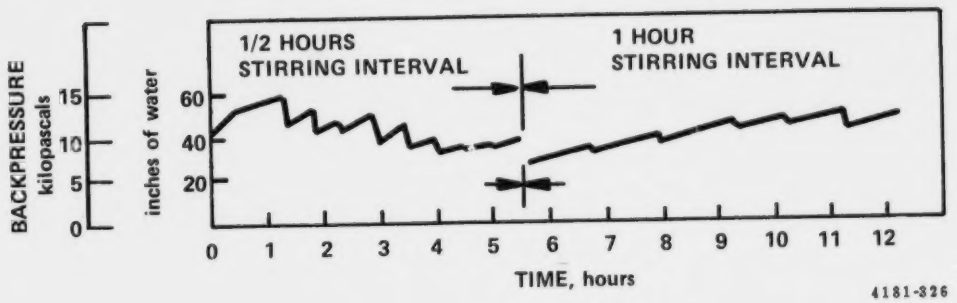

Figure 26. Gravel bed filter backpressure with stirring.

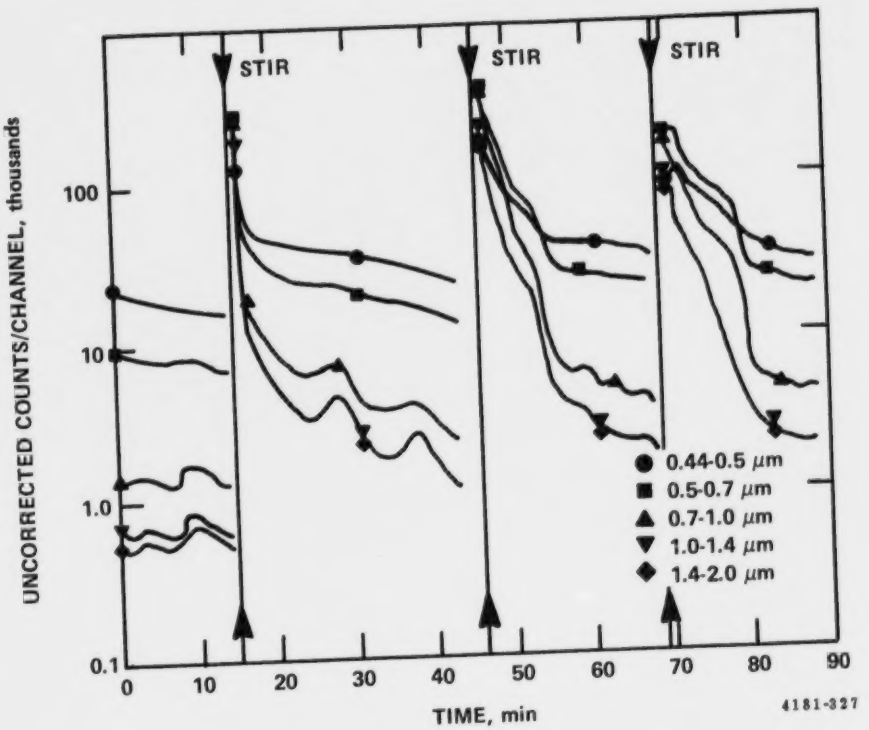

Figure 27. Gravel bed filter output with stirring at 30 minute intervals.

TABLE 2. SUMMARY OF GRAVEL BED FILTER TESTS

Date	Configuration	Efficiency (%)	ΔP(kPa)	Remarks
7/02/80	5 cm 1mm shot updraft	5	-	Drop in backpressure due boiling of shot in 3 places. Shot bed solidified upon cooling.
7/02/80	5 cm 2mm shot updraft	22	5.4	No boiling of shot.
7/03/80	5 cm 2mm shot updraft	7	6.8	Shot boiling in 3 places after 6 hours.
7/07/80	10 cm 2mm shot downdraft	46 60	6.8 17	Efficiency increases with backpressure. Ref. Figure 25.
7/09/80	10 cm 2mm shot downdraft	- 72	12 27	Continuation of previous test. Backpressure lower initially due to stirring of shot. Ref. Figure 25.
7/11/80	10 cm 2mm shot downdraft	40 ave	12 ave	Stir shot every 0.5 hour. Ref. Figures 26 and 27.
7/14/80	10 cm 2mm shot downdraft	33 ave	12 ave	Stir shot every hour. Ref. Figure 26.

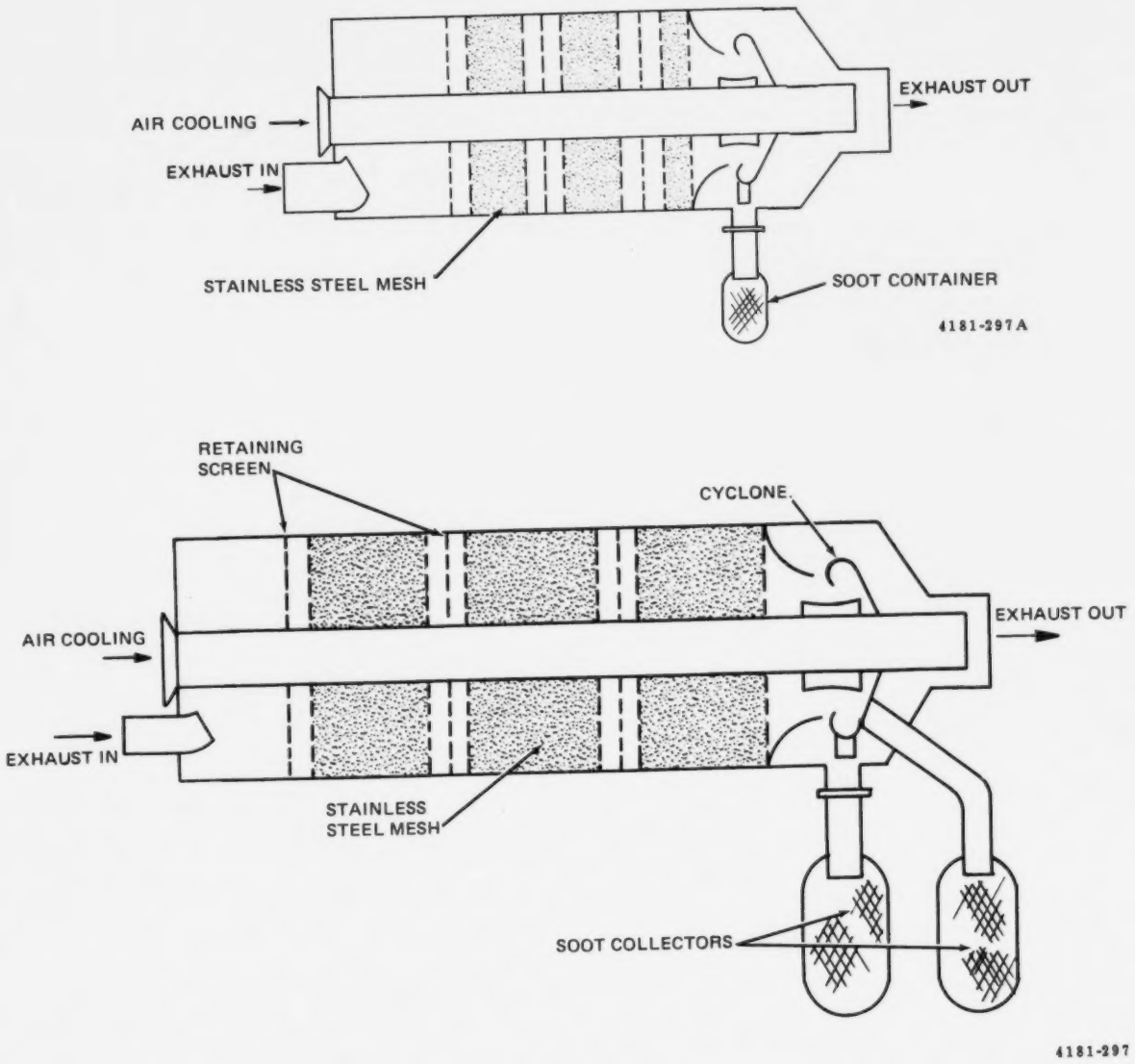

Figure 28. Cross section and relative sizes of medium and large capacity Aut-Ainers.

tube and sandwiched between perforated plates. The device depends on cooling condensation for agglomeration and collection of particulate matter. The cooling is supplied by the central tube which acts as a ram air tube. Heat transfer is augmented by several perforated plates located across the gas flow and connected to the cooling tube. The exhaust gas flow is expected to tear agglomerates off of the wire mesh and swirl them through the cyclone to a catch bag located on the side of the device, resulting in an effectively self cleaning device. The only service required would be periodic changing of the soot collection bag.

Two models of Aut-Ainers were tested. The first was the smaller one shown in Figure 28 in which the first two bands of steel mesh are 5 cm thick and the third is 2.5 cm thick. The mixing of the cooling air with the exhaust at the end of the Aut-Ainer initially caused some concern as the effects on the condensable hydrocarbons in the exhaust stream were unknown. This difficulty was overcome by extending the cooling air tube down the center of the sampling port tube so that undiluted exhaust could be sampled. After this, a baffle was placed in the exhaust pipe to promote mixing and another sampling tube was placed downstream to allow sampling of the diluted exhaust. The amount of dilution present was determined by examining the concentrations of CO, CO_2, and NO_x present before and after dilution and deriving a correction factor based on the assumption that the quantities of these gasses were invarient. Outlet EASA and filter sampling were performed on both diluted and undiluted gas streams. Outlet impactor data were obtained from the diluted flow only.

The second Aut-Ainer tested was designed after the first test was completed in the belief that a larger design would be more suitable for an engine of 5.7 liter displacement. This device is essentially the same as the smaller one except that the three sections of mesh are 18 cm long for a total of 54 cm and that there is a bleed-off pipe connected to the back of the cyclone. This is the larger device shown in Figure 28. The outlet used a double pipe arrangement which carried the cooling air past the sampling ports before allowing mixing. The catch bags were enclosed so that the exhaust through the bags could be examined. The flow rates in the inlet and regular outlet were close to 7.6 actual m^3/min (270 acfm) which gives a velocity through the filter of 2.1 m/sec. The flow through the bags barely registered on the water manometer used with the pitot tube. Based on an estimated 0.13 cm (0.05 inch) deflection, a flow rate of 0.9 actual m^3/min (31 acfm) was obtained. This is only 14% of the total flow.

A condensation trap designed by the University of Tokyo was also tested. This device, shown in Figure 29, has no air pipe but is designed to maximize its surface area for cooling purposes. The device is 5 cm thick by 40 cm wide and contains

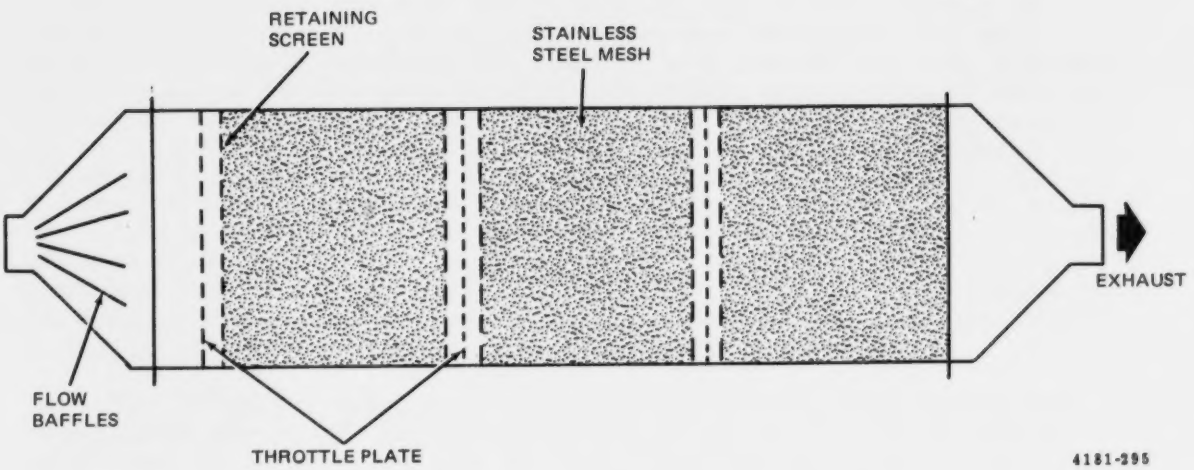

Figure 29. Flat Condensation Trap.

three 27 cm long sections of the same steel mesh. There is no cyclone in this device and therefore any agglomerates which are formed on the wire mesh and subsequently reentrained should be discharged through the exhaust outlet. The device was built for a 1 liter engine having a maximum gas flow rate of 3.5 m^3/min. Consequently, the truck was run at 32 km/hr which gave a gas flow of about 3.2 m^3/min and a filtration velocity of 2.7 m/sec.

Test Results

The first Aut-Ainer was examined at DOT. According to the manufacturer, who was at DOT for the first week of testing, the Aut-Ainer requires about 12 hours of running-in time to obtain maximum efficiency. Therefore, after the final testing configuration was achieved, the remainder of the first week was spent running the engine to accumulate hours on the Aut-Ainer and checking out test equipment. During this period, the engine speed was 1700 rpm (∿88 km/hr or 55 mph) which corresponds to a linear velocity through the filter of 2.9 m/sec. After 20 hours of running, an efficiency of 12% was obtained for this speed. The manufacturer also pointed out the device was designed for an engine in the 2-3 liter displacement range rather than the 5.7 liter engine being used. By scaling speeds and displacements, 48 km/hr (900 rpm) on the 5.7 liter engine can be considered the equivalent of the desired test speed of 88 km/hr (55 mph) for a 3 liter engine. Therefore a test was run at 900 rpm which yielded an efficiency of 32%. The efficiencies quoted are overall figures derived from filter and impactor data. Ultrafine data indicate that the device was condensing but not collecting large quantities of small particles. Figure 30 shows impactor and EASA derived particle collection efficiencies for both engine speeds.

The large capacity Aut-Ainer was tested at SoRI using the conditions for which it was designed, i.e., a 5.7 liter vehicle operating at 88 km/hr. Filter data taken at the regular gas outlet indicated that the device was collecting 35% of the particulate after 40 hours of operating time. EASA data taken at this point showed a negative efficiency for particles of less than .7 μm diameter, which suggests that this device, like its smaller counterpart, was condensing vapors to form small particles.

The filter samples taken from the exhaust through the catch bags were pale yellow. This implies that only negligible quantities of soot passed these bags which would indicate a high efficiency if opacity measurements were made. However, these filters showed a larger weight gain than the very black filters taken from the regular exhaust. The collection efficiency through the bags measured 22% with negative efficiency again occurring for the small particles. The temperature of the gas at this point was 84°C (184°F) compared to 132°C (271°F) at the regular outlet and 174°C (345°F) at the inlet. Since the temperature was less than 100°C,

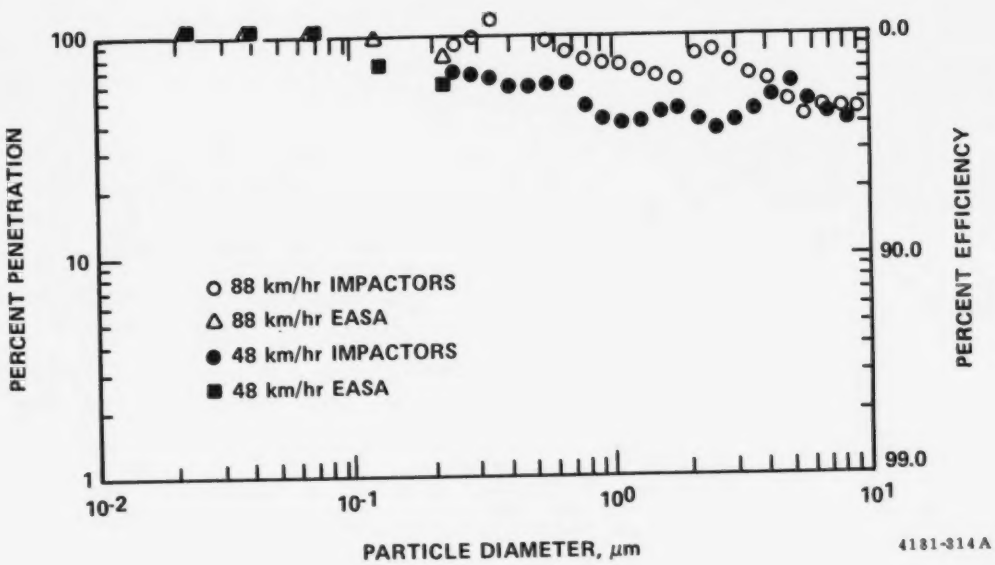

Figure 30. Aut-Ainer efficiency for 88 and 48 kph speeds.

the filters were desiccated for several days and reweighed. The changes in weight were within the error of the weighing procedure which suggested that the weight gain was due to condensed hydrocarbons. Figure 31 shows gas chromatography data taken from the residue collected on the filters. Although the individual peaks are not identified, a shift toward lighter, lower condensation temperature organic compounds is evident in the sample taken from the catch bag exhaust filter. This reinforces the probability that the weight gain on this filter is due to condensed hydrocarbons.

The University of Tokyo condensation trap was run at a reduced speed to reduce the gas flow rate to the 3.2 m^3/min for which the device was designed. After 20 hours of operation the efficiency was 36% with a backpressure of less than 3 kPa (12 in. H_2O). EASA data indicate that the device is not agglomerating at all but is producing a condensation fog of very small particles.

Table 3 summarizes the testing of the three traps. The pressure drop across these devices ranged from 2 to 5 kPa (8 to 20 inches of water), which is lower than for the other mechanical collection devices tested. Since the medium capacity Aut-Ainer was tested at DOT, several different sampling techniques were used. There was good agreement between the different systems except for the EASA which examines only a very limited range of particle sizes and therefore cannot be used to determine overall efficiency values. For the tests performed at SoRI, only mass filters and the EASA were available for particle sampling.

Conclusions

The three condensation traps tested were unable to achieve acceptable collection efficiency levels. In addition, there was no evidence that these devices were agglomerating particles. Instead, they produced a fog of small particles as hydrocarbon vapors present in the diesel exhaust were condensed in the control device.

CERAMIC BARRIER FILTER

A Corning ceramic monolith of the type used for catalyst substrates was tested at DOT. This device, which was a 15 cm diameter cylinder having a length of about 18 cm, was a honeycomb of square thinwall tubes of about 1.5 mm on a side. These tubes, which ran the length of the element, were alternately blocked at each end so that the gas flow would have to pass through the walls of the tubes. This device was tested at 900 rpm (~48 km/hr or 30 mph) in a holder which supported its outer wall as a previous sample tested at 1700 rpm with unsupported walls had exploded. The ceramic filter showed collection efficiencies of 92% using impactors and 97% using the EASA. As shown in Figure 32, the

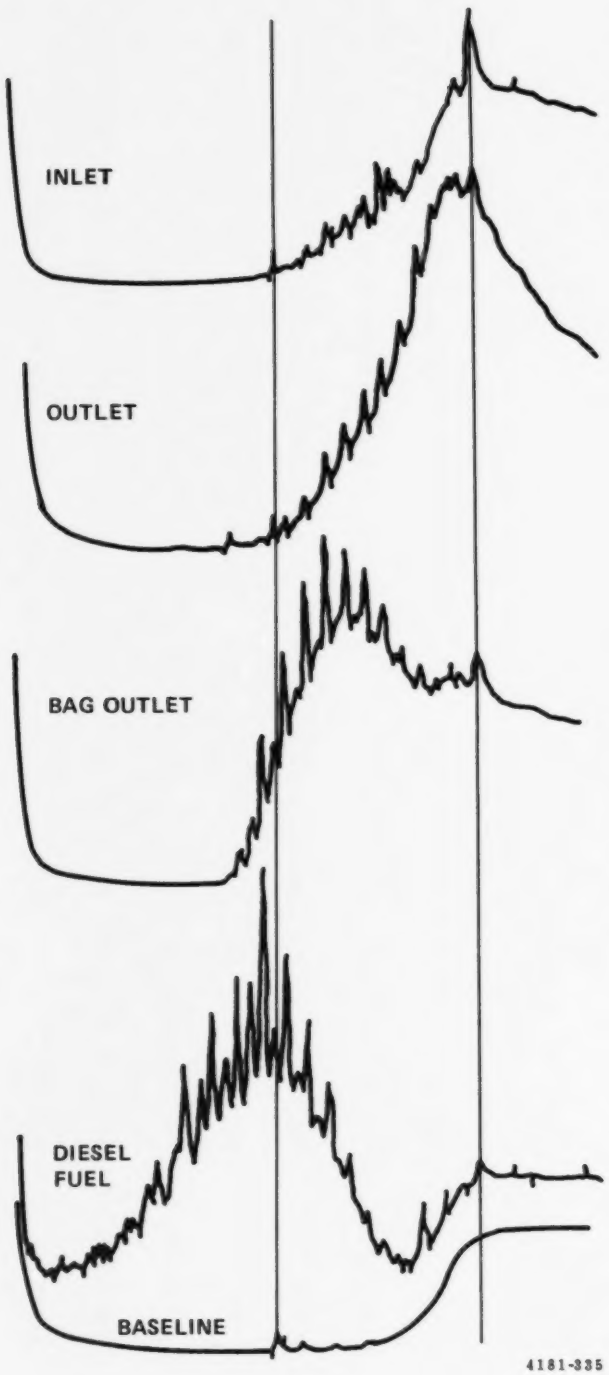

Figure 31. Gas chromatogram of residue from filters taken during the large Aut-Ainer test.

TABLE 3. SUMMARY OF CONDENSATION TRAP TESTS

Test Location & Date	Engine Conditions	Device	% Efficiency: Dilution Tunnel	Mass Filter	Cascade Impactors	EASA	NOTES
DOT 5/1/80	1700 rpm	Medium capacity Aut-Ainer	25	-	31	-	Device disassembled, inspected, and reassembled after test. Backpressure is 4 kPa.
DOT 5/2/80	Same	Same	26	-	15	-	Device run all day to accumulate hours.
DOT 5/5/80	Same	Same	15	13	9	<0	Backpressure is 5 kPa.
DOT 5/5/80	900 rpm	Same	-	25	39	20	Total run time 20 hours. Backpressure is 2 kPa.
SoRI 7/25/80	88 km/hr	Large capacity Aut-Ainer	-	27	-	-	Backpressure is 2 kPa.
SoRI 7/29/80	Same	Same	- -	35 23	- -	<0 -	Lower figure is from data taken on collection bag outlet.
SoRI 8/04/81	Same	Same	-	34	-	<0	Total run time 40 hours. Backpressure is 5 kPa.
SoRI 5/27/81	32 km/hr	Small capacity flat trap	-	38	-	-	Backpressure is 2.5 kPa.
SoRI 5/28/81	Same	Same	-	36	-	2	Total run time 20 hours.

56

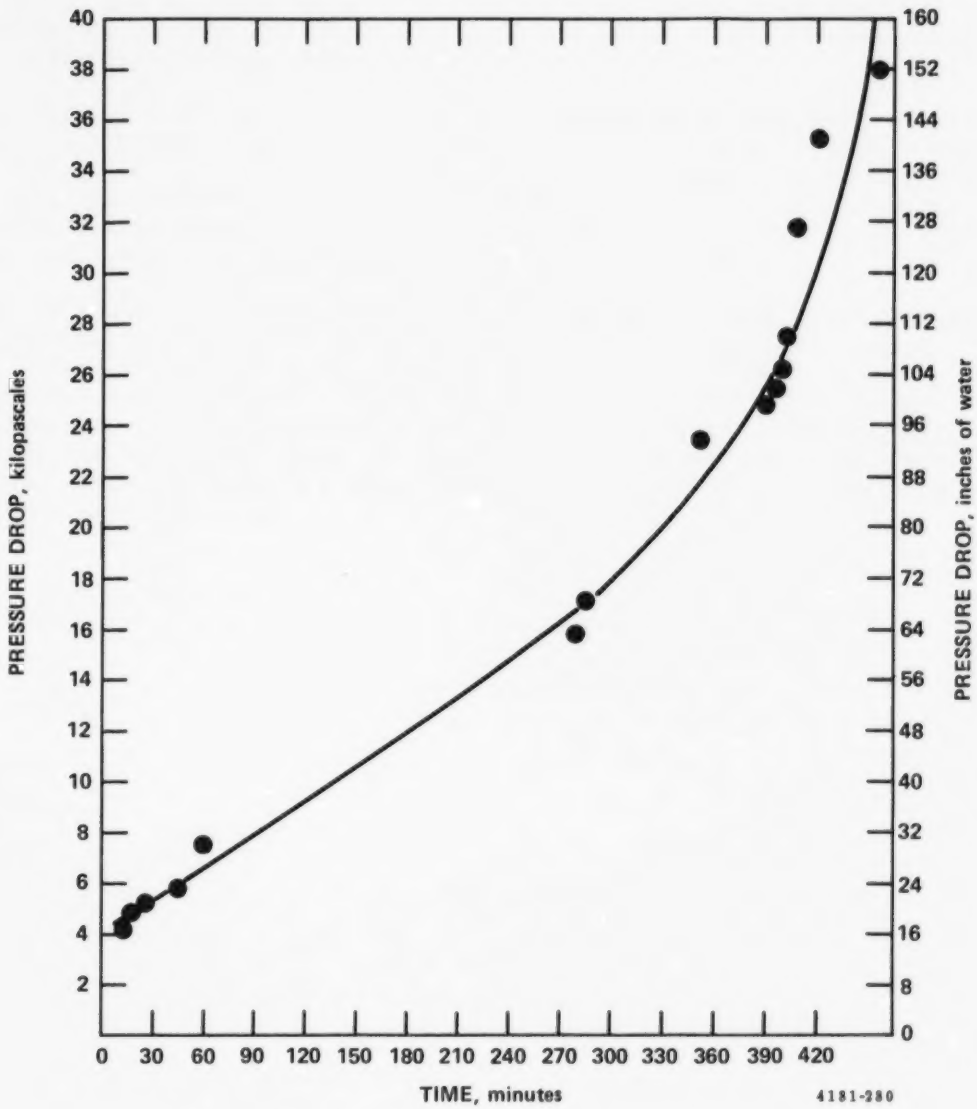

Figure 32. Pressure drop across Corning ceramic filter (DOT data, 5/9/80).

backpressure rose quickly and reached a pressure of 35 kPa (140 in. H_2O) after seven hours of operation.

COOLED EXHAUST LINE

A series of exhaust line cooling experiments were conducted in order to test whether the performance of aftertreatment devices might be improved by controlling the temperature of the exhaust gas. Both the agglomeration of diesel soot particles and the condensation of hydrocarbons on the particles might be enhanced by cooling the exhaust gas.

Standard 6.25 cm (2.5 inch) OD exhaust pipe was formed into a series of loops through two 210 liter (55 gallon) drums. The level and flow rate of tap water in the two drums was varied to stabilize the outlet exhaust gas temperature at various values. Mass train measurements on samples of the exhaust gas were carried out at the inlet to and outlet from the water drums.

Mass loading data are plotted in Figure 33 for four exhaust gas temperatures between 48°C and 93°C. The inlet and outlet mass loadings are the same, within experimental error, except at the highest temperature. There is no evidence of substantial condensation of hydrocarbons onto particles in the gas stream. Condensation occurred only on the cooled pipe walls. The cooling apparatus was not used in the subsequent testing of diesel exhaust aftertreatment devices.

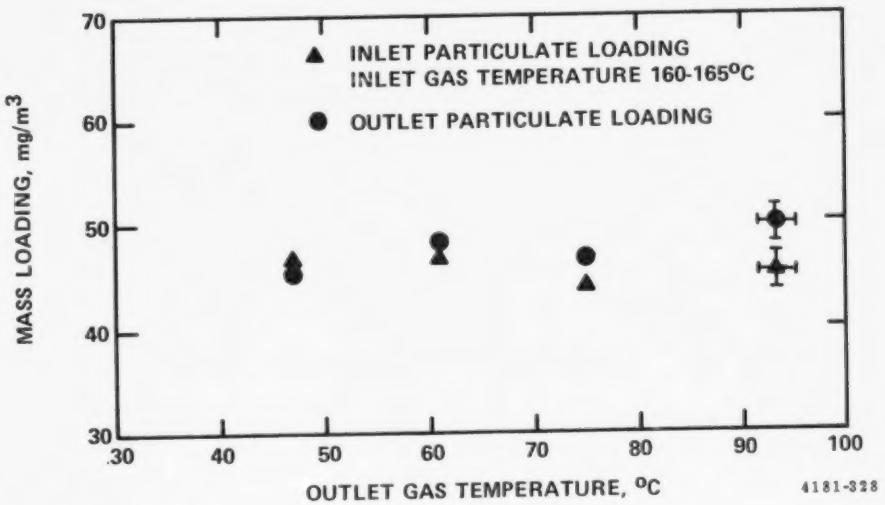

Figure 33. Hydrocarbon condensation on diesel soot as a function of temperature.

SECTION 6

ELECTROSTATIC PRECIPITATORS

CYLINDRICAL ELECTROSTATIC PRECIPITATOR

Electrostatic gas cleaning technology was applied to the aftertreatment of diesel exhaust with a specially designed electrostatic precipitator (ESP) developed by SoRI. Electrostatic precipitation has the possible advantage of high-efficiency collection of submicron diesel particles with low engine backpressure and the expenditure of low electrical power. On the other hand, the low resistivity of the diesel particulate matter leads to the possible difficulties of surface current leakage through sooty deposits on insulators and poor particle adhesion to the collection plates.

The ESP is a cylindrical, two-stage device. Particle charging and collection functions are separated in order to design maximum collecting plate area in a small volume of space. The ESP is designed to be periodically wet-flushed in a vertical orientation. A schematic diagram is given in Figure 34.

Charging Section

Five star-shaped sets of corona points are mounted on a vertical high-voltage rod chosen for mechanical strength. The corona electrode is typically operated at 40 kV (negative) and about 250 μA. The internal diameter of the ESP is 20 cm (8 in.). A volume gas flow of 6.2 actual m^3/min (220 acfm), at a truck speed of 88 km/hr (55 mph), gives an average linear gas flow down through the ESP of 3.2 m/sec (10.5 ft/sec).

The product of negative ion density and particle charging time in the corona section is

$$N_0 t \simeq 0.6 \times 10^{13} \text{ sec/m}^3,$$

at an electric field of approximately 4×10^5 volt/m.

Collecting Section

The collector is a set of concentric cylinders (overlapping length 28 cm (11 in.) alternately grounded and biased negative).

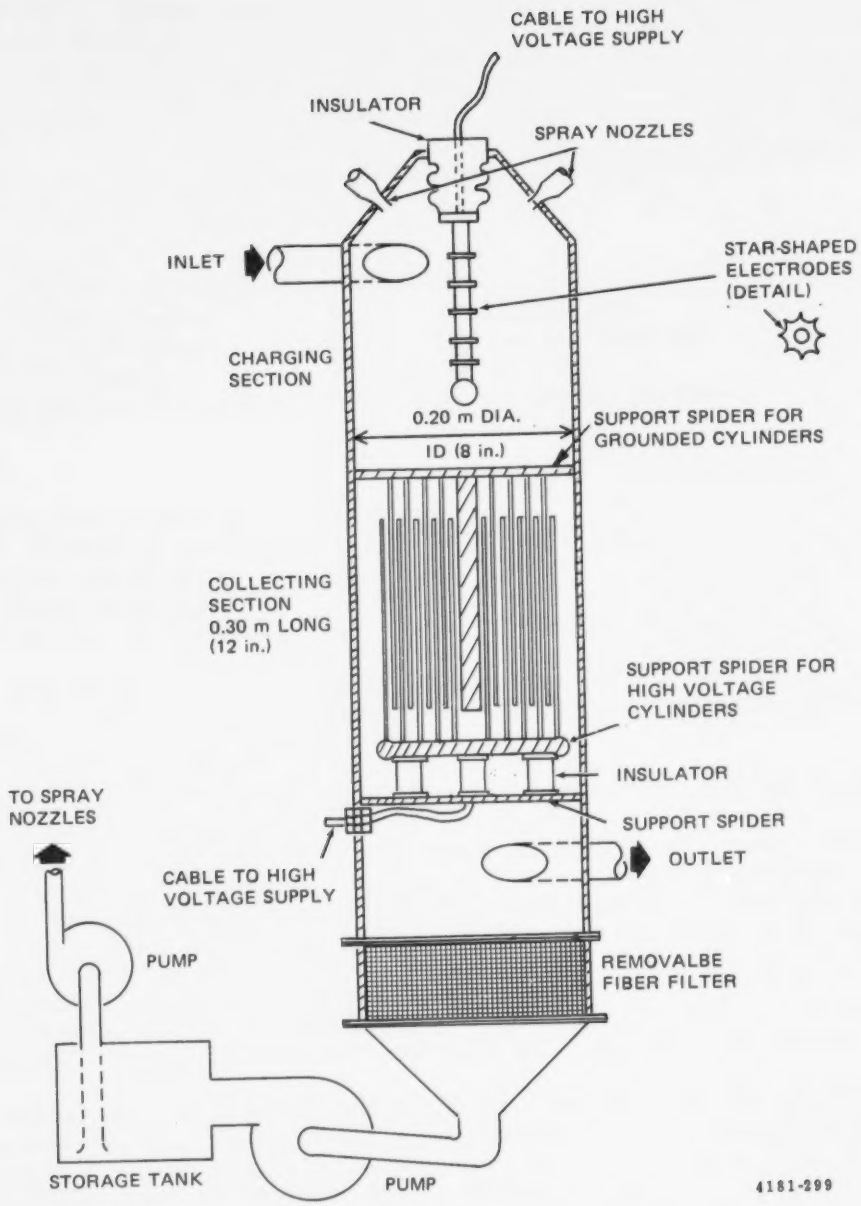

Figure 34. Schematic diagram of the precipitator.

The total collecting area is 1.18 m^2 (12.7 ft^2). For the volume flow of 6.2 m^3/min, the specific collection area is about 11.3 $m^2/(m^3/sec)$(58 ft^2/1000 ACFM).

The collector cylinders have a nominal spacing of 0.6 cm (1/4 inch). After wet-flushing loose particles, the cylinders will hold about 6 kV without arcing. In order to increase the collecting electric field, the voltage is increased to typically 15 kV, with steady arcing carrying about 1.5 mA. Then the collecting electric field is about 24 x 10^5 volt/m.

Two tests of the ESP are summarized below.

Test 1

Mass sampling period	6 hours
Engine backpressure	5 kPa (20 in. H_2O)
Collector cylinders	6 kV, 500 µA to 950 µA
Inlet mass loading	58 mg/m^3
Mass removal efficiency	40% (see comments below)

Test 2

Mass sampling period	6 hours
Engine backpressure	5 kPa (20 in. H_2O)
Collector cylinders	20 kV, 2 mA
Inlet mass loading	66 mg/m^3
Mass removal efficiency	42% (see comments below)

These tests were conducted with the diesel truck running at 88 km/hr (55 mph). The exhaust gas temperature at the truck outlet was 170°C to 175°C (340°F to 350°F).

When the collector cylinders were maintained at high voltage below the sparking level (Test 1) the variations in collector current indicated buildup and reentrainment of sooty deposits on the collector cylinders. There was little accumulation of diesel soot on the insulators and the ESP was operated for about 40 hours (the last 20 hours in connection with a large industrial cyclone) without cleaning. The mass train sampling in Tests 1 and 2 was of a preliminary nature and was not isokinetic. Later measurements (with cascade impactors and a backup filter) of the mass removal efficiency of the ESP gave values of about 26%.

While the ESP achieved only low collection of diesel soot, there was on the other hand a substantial agglomeration of the particles. Electrical aerosol size analyzer data for Tests 1 and 2 are displayed in Figure 35 in terms of mass removal efficiencies in the small size ranges. The data for 20 kV on the collector cylinders (Test 2) show 60% to 70% removal of particles of aerodynamic diameter on the order of 0.1 µm. In addition, the mmd

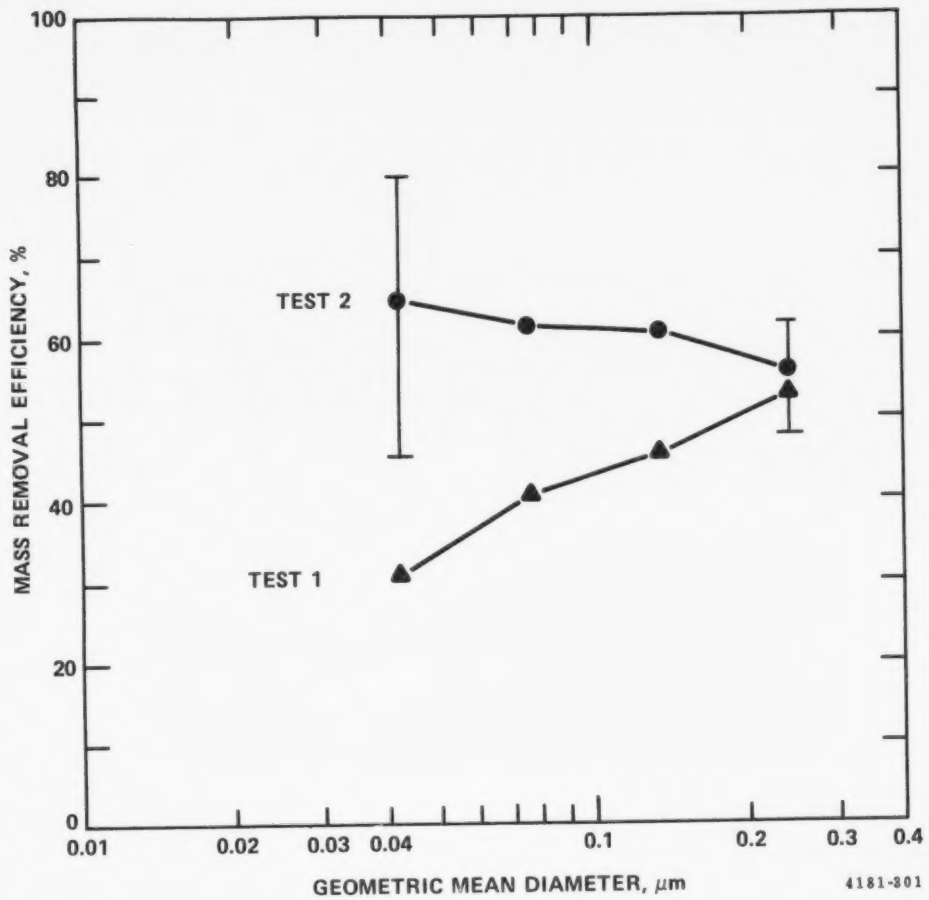

Figure 35. Removal of diesel particulate from small size ranges by electrostatic precipitation.

of the effluent particles was increased by an order of magnitude. The agglomeration phenomenon was easily confirmed by visual observation of some macroscopic agglomerates. Microscopic examination of a sample of particles from the ESP outlet showed a preponderance of very loose and fluffy agglomerates the order of 25 μm in actual size. (Settling velocity experiments with large agglomerates indicated that the aerodynamic diameter was roughly one-tenth the actual particle size. This was consistent with later cascade impactor measurements of the mmd at the ESP outlet.)

Conclusions

Further testing of the ESP was designed to emphasize its role as an agglomerator, with the ESP followed by some other device for trapping the agglomerated diesel soot.

DIESEL PARTICULATE RESISTIVITY

The electrical resistivity of the diesel soot is of concern in regard to surface conduction through sooty deposits on insulating standoffs in the ESP. In the course of the preliminary experiments with the ESP, a bulk sample of agglomerated diesel soot was accumulated in the bottom of the ESP. These particles were sufficiently large that they did not follow the exit gas stream. (These particles contribute to the 26% mass removal efficiency of the ESP along with the small permanent collection of diesel soot on the collector cylinders.) Laboratory resistivity measurements were performed on this sample.

The diesel particulate resistivity was measured in moist air using an ASME PTC-28 test cell. The fluffy soot was compacted as little as possible, only to the extent of resting the upper electrode on a sample 0.39 cm thick. Results are given in Table 4. With temperature and moisture content comparable to that of the diesel exhaust gas, the resistivity of the fluffy agglomerated soot measured about 10^7 ohm-cm.

The layer of diesel soot impacted on the half-inch diameter insulating standoff to the corona electrode of the ESP was estimated to be no more than 0.25 mm thick. Using the measured resistivity of the soot, the corona leakage current across the insulator was estimated to be less than 20 μA.

ESP CLEANING FLUIDS

The ESP was designed to be periodically wet-flushed in a vertical orientation. Several common cleaning fluids (and also diesel fuel) were bench-tested for effectiveness in flushing diesel soot. The fluids were tested both on bulk samples of soot and on soot layers impacted on the metal housing of the deep bed filter. Subjective judgements of relative effectiveness

TABLE 4. DIESEL PARTICULATE RESISTIVITY

Temperature °C	Moisture Volume %	Voltage volts	Average Field kV/cm	Resistivity ohm-cm
148	0	50	0.13	9.0×10^7
149	6.3	50	0.13	7.8×10^7
151	15.0	50	0.13	4.1×10^7
151	15.0	100	0.26	3.7×10^7
151	15.0	500	1.28	1.9×10^7
151	15.0	1000	2.56	1.2×10^7
151	15.0	2000	5.13	Dielectric failure

were translated onto a scale of zero to ten and are presented in Table 5. The three chlorinated hydrocarbons were roughly equivalent in effectiveness. Perchloroethylene, a common dry cleaning fluid, was chosen for cleaning the ESP because it is effective, nonflamable, and of relatively high boiling point and low toxicity.

Occasional flushing of the ESP was done in a well-ventilated laboratory, after the device had cooled down overnight. About 4 liters (1 gallon) of perchloroethylene was pumped (with a battery operated fuel pump) directly from a supply container through four spray nozzles in the top of the ESP. The dirty fluid flowed directly from an outlet in the bottom of the ESP into a take-up container. Teflon insulators were thoroughly cleaned, but there always remained a thin film of soot on metal surfaces which could not be removed by any cleaning fluid (without rubbing).

One problem in the aftertreatment of diesel exhaust is the collection and handling of the large volume of low bulk density soot (roughly 120 kg/m^3). An advantage of wet flushing with perchloroethylene is that the collected soot is left in a highly compacted state when the dirty cleaning fluid is evaporated (to be followed by condensation in a closed system). The bulk density of dry residue from the wet-flushing procedure was measured to be 1300 kg/m^3. Consequently, the collected particulate storage volume required for an 8000 km (5000 mi) service interval would be reduced to 3 liters ($\sim$0.1 ft^3).

MOVING BELT ELECTROSTATIC PRECIPITATOR

A moving belt electrostatic precipitator (MBP) designed for automotive use was also tested. Figure 36 shows a sketch of the device. It is designed to be self-cleaning by means of a moving belt type collection plate. As the belt passes around a roller at each end of the device, the collected soot is compressed. The compressed soot is then removed from the belt and rollers by a set of scrapers which are positioned so that the dislodged soot will fall through a hole in the bottom of the device into a receptacle. The self-cleaning feature is supposed to reduce reentrainment by preventing an appreciable accumulation of collected soot in regions where it would be subjected to high gas velocities. The electrodes for the charging wires pass through the exhaust ports for reduced fouling. The overall size of the device is 148 x 20 x 75 cm high. The collection cavity measures 84 x 6 x 31 cm high.

Operation

In order to test this device it was necessary to sample the inlet and outlet gases without introducing uncertainties such as

TABLE 5. EFFECTIVENESS OF DIESEL SOOT FLUSHING FLUIDS

Flammable		Non-Flammable	
Fluid	Flash Point °C	Fluid	Boiling Point °C
		Trichloroethylene	87
		Perchloroethylene	121
		Carbon Tetrachloride	77
Mineral Spirits	40		
Acetone	-18		
Kerosene	-40		
Ethyl Alcohol	13		
Benzene	-11		
Diesel Fuel	- 4		
		Detergent	100

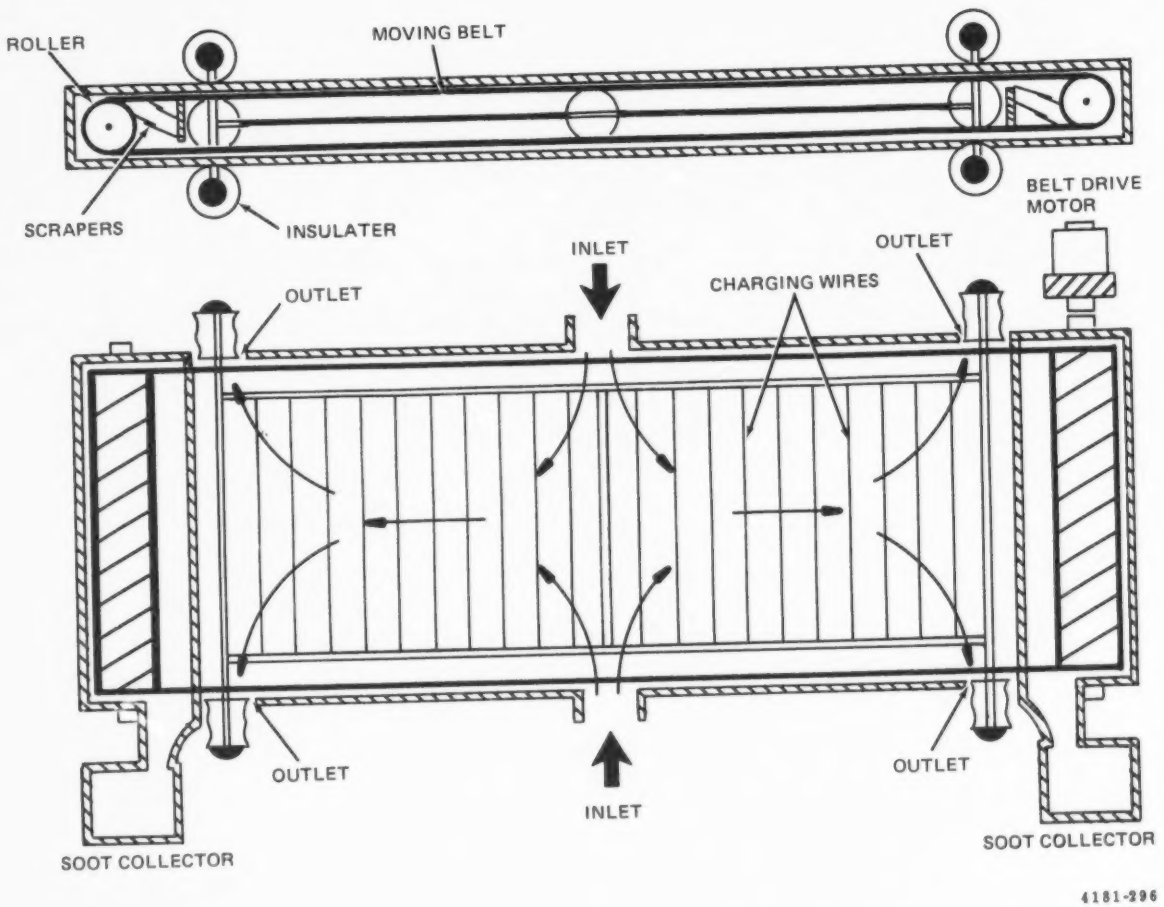

Figure 36. Moving belt electrostatic precipitator.

dilution of the outlet gas with an unknown quantity of ambient air. For this reason a complicated array of exhaust pipes was fabricated to split the inlet gas into two streams as required by the device, and to recombine the four outlet streams into one for gas sampling. Since the four high voltage electrode support rods pass through the center of the four gas outlets, it was necessary to use sections of teflon pipe in the outlet plumbing to provide electrical insulation. This arrangement increased the susceptibility to current leakage through soot deposits thereby limiting the achievable operating voltages.

The device was designed for use following the flat condensation trap used as an agglomerator. Tests in Japan were performed on a simulated agglomerated soot (0.9 μm mmd) produced by burning natural gas with excess air.[20] For a 2.7 m^3/min gas flow rate at 40°C, collection efficiencies of 60% (stationary belt) and 82% (moving belt) were measured. However, since tests at SoRI had shown that the condensation trap did not agglomerate particles, it was not used when SoRI tested the MBP. At SoRI, the MBP was tested on untreated diesel exhaust having a particulate mmd of 0.3 μm. The 32 km/hr (20 mph) truck speed resulted in a gas flow rate of 3.2 m^3/min, which is less than the rated maximum of 3.5 m^3/min for this device. The gas temperature was 113°C, resulting in a drier, more easily reentrained soot. Tests were also conducted at flow rates of 2.0 and 2.5 m^3/min.

Operation of the moving belt precipitator revealed several mechanical problems associated with the belt drive mechanism. Since the belt-roller system was not designed to be self-centering, the belt would walk off the end of the roller. When this occurred, the edges of the belt would develop small cracks until pieces of belt were broken off and the belt jammed and stalled the belt drive motor. On some occasions when the belt jammed, it could be restarted by prodding the belt drive gears with a screwdriver. On other occasions, it was necessary to dismantle the MBP, recenter the belt by hand, and reassemble the MBP. Since there was no way to determine when the belt tension was optimized to minimize belt walking, the belt had to be positioned several times before the test was completed. On one occasion, the belt was trimmed to remove the cracked edges.

Under static conditions, the MBP would support 20 kV on the charging assembly without sparking. The Japanese data were obtained using 18 kV. Under actual operating conditions at SoRI, the maximum achievable voltage at the high flow rate was 15 kV at about 9 mA. For the lower flow rates, however, the voltage dropped to 8.5 kV due to higher leakage currents resulting from contamination of the insulators with conductive soot particles. Figure 37 shows the voltage-current curves for this device under static and high flow rate conditions. The displacement of the curve taken under operating conditions is due to current leakage.

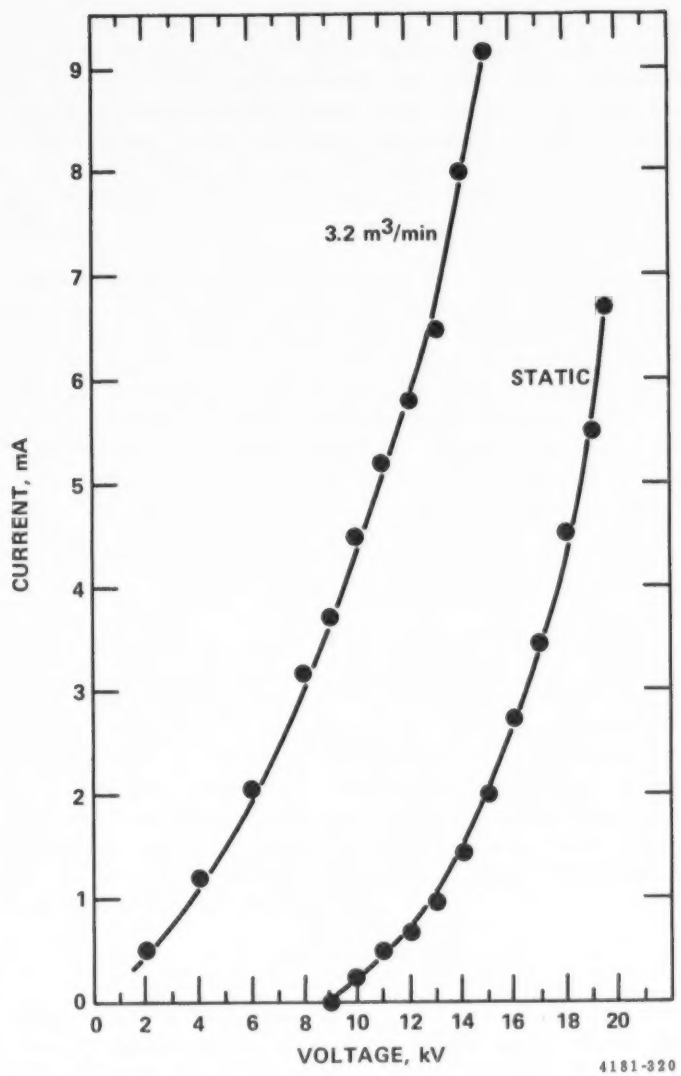

Figure 37. IV curves for moving belt electrostatic precipitator.

The first tests with this device were made at the high flow rate (3.2 am^3/min) with the belt stationary. The belt was run briefly once every five minutes to reduce the thickness of the dust layers. After two hours of testing with intermittent belt operating, testing was begun with continuous belt operation. After 14 minutes, the belt jammed but could be restarted by prodding the drive gears with a screwdriver. After this it was necessary to set the belt drive motor control to 50% speed to keep the belt from stalling. The belt speed at this setting appeared to be about that obtained at the 20% setting before the belt jammed, which indicates that the belt was still rubbing on the MBP housing. The belt jammed several times during testing until, on the second day of operation, it could not be restarted by prodding the gears. At this point testing at this flow rate was terminated.

Before the device could be tested further it was necessary to disassemble it and reposition the belt. When the precipitator was dismantled, it was observed that a heavy coating of soot had increased the apparent size of the corona wires to about 0.3 cm (0.12 in.). This coating was fragile and could be broken loose by lightly jarring the corona discharge assembly. A coating of soot was also observed on the teflon insulators. Current leakage through this deposit undoubtedly proved to be a major factor in limiting the operating voltage. By contrast, no soot had adhered to the moving belt and very little soot was found in the soot containers. Apparently the collected soot was dislodged by the flexing and buckling of the belt and reentrained into the gas stream.

The testing at the lower flow rates was performed with a stationary belt which was periodically rotated to dislodge any collected soot. The belt, which had become stretched out of shape, was then carefully positioned so that the one large buckle present would be supported on a roller thereby allowing maximum wire-to-plate spacing. Severe current leakage problems appeared very quickly and the operating voltage was limited to a maximum of 8.5 kV. Inspection of the insulators after the termination of testing showed a thicker layer of soot than had been deposited during the high gas flow tests.

Test Results

Filter data taken during the initial period of testing, with intermittent belt operation and the high gas flow rate, yielded a collection efficiency of 9%. The data taken over the testing period when the belt was moving reduced to a 21% collection efficiency. EASA data taken during these tests indicated a positive efficiency for particle sizes less than 0.1 μm but a zero or negative efficiency for particles in the 0.2 and 0.75 μm size range for both the intermittent and the continuously operating conditions. These data are shown in Figure 38. Filter data for

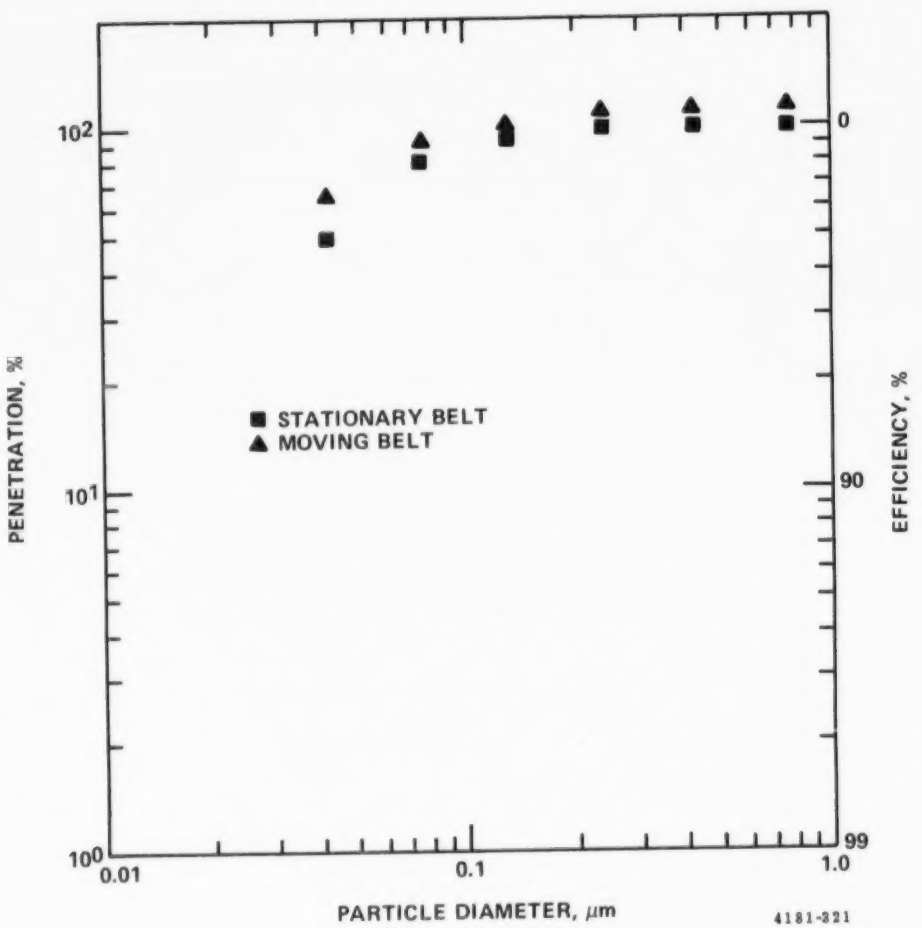

Figure 38. Efficiency of the moving belt precipitator for the small particles.

the low flow rates yielded 13% efficiency for a flow rate of 2.0 am^3/min and 9% for 2.5 am^3/min. However, due to the reduced electric fields present in the low flow rate tests, these values are difficult to compare to other test data.

Conclusions

The moving belt ESP showed very low efficiencies at its rated maximum gas load when used with actual diesel particulate. In addition, it does not appear to be sufficiently reliable in operation to be used on diesel vehicles.

SECTION 7

COMBINED ELECTRICAL AND MECHANICAL DEVICES

ELECTRIFIED FILTER

The concept of agglomerating and trapping diesel particles in a single compact device was tested with an electrified filter. A schematic diagram of this device is given in Figure 39. The design features of this device are:

(1) Particle charging and collecting functions are separated. A disc electrode in the charging section is kept clean by a high gas flow (about 36 m/sec at 6.2 actual m^3/min (220 acfm), for a vehicle speed of 88 km/hr). In the collecting section, the high axial gas flow is converted into a much lower radial gas flow (about 0.6 m/sec) through the collector screen and filter material.

(2) Fiber filtration in the collecting section is enhanced by the superimposed electric field. Both electrical and mechanical collecting forces are effective.

(3) The fiber filter can be formed as a replaceable cartridge. Collection and removal of the diesel particulate can be accomplished simply by replacing the filter cartridge.

Possible disadvantages of the design include (1) the degradation of electrical energization of the collecting section due to the buildup of conducting sooty paths through the filter material and (2) the buildup of engine backpressure due to a cake of particulate matter forming on the filter.

Corona Electrode

The corona electrode was a single, half-inch diameter metal disk with sharpened edge. The disk was mounted in the center of the 6.0 cm ID exhaust gas inlet pipe. The corona electrode was operated at 20 kV and about 350 μA steady current. No fouling of the corona electrode insulator by diesel soot was experienced. The product N_0t of negative ion density and particle charging time was estimated at about 10^{12} sec/m^3. For saturation charging of the diesel particulate, this parameter is low by about an order of magnitude.

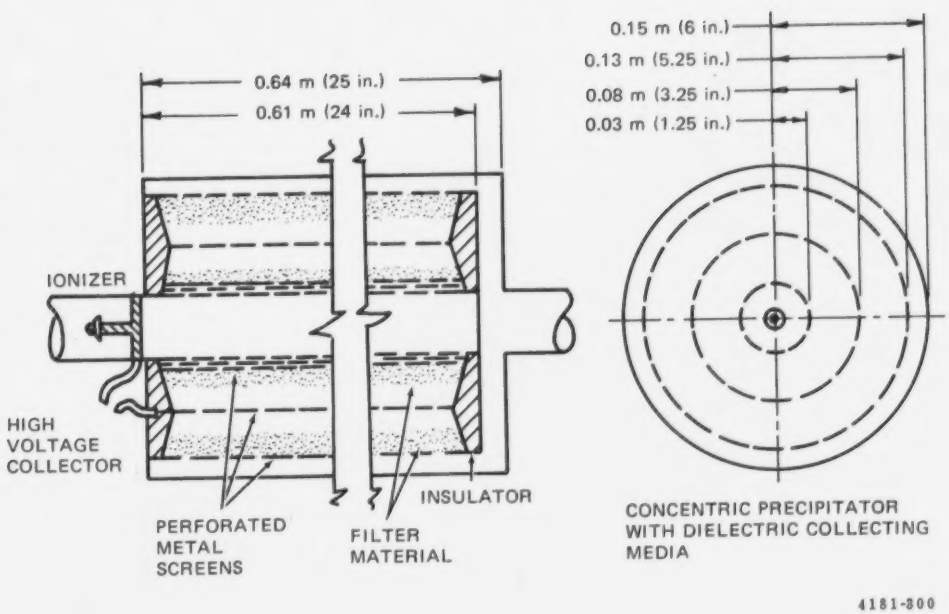

Figure 39. Schematic diagram of the electrified filter.

Collector Electrode

The collector electrode was a cylindrical, perforated metal screen, 16.5 cm (6 1/2 inches) in diameter by 56 cm (22 inches) long, of open area 58%. All testing of the device was conducted at a diesel truck speed of 88 km/hr (55 mph). The exhaust gas temperature at the truck outlet was 170 to 175°C (340 to 350°F).

Test Results

Test 1:

Fiberglass angel hair was loosely packed on either side of the collector screen to an average open volume (by mass density) of 98%. The angel hair was found to be sufficiently conductive to form an electrical short in the collecting section, and this arrangement was not tested further.

Test 2:

The device was operated with no filter material in the collecting section and tested by mass train sampling at the inlet and the outlet. The test data are summarized below.

Mass sampling period	2 1/2 hours
Engine backpressure	3 kPa (12 in. H_2O) steady
Collector screen	20 kV, steady; 0.5 mA to 2 mA
Inlet mass loading	63 mg/m^3
Mass removal efficiency	32%

Variations in collector current indicated buildup and reentrainment of sooty deposits. The device was disassembled and thoroughly cleaned between tests.

Test 3:

The inner and outer spaces of the collecting section were loaded with strips of fiberglass thermal insulation oriented with the radial gas flow parallel to the fiberglass layers. This arrangement was intended to enhance penetration of diesel soot into the filter rather than formation of a cake on the surface. The test results are summarized below.

Mass sampling period	1 hour
Engine backpressure	3.0 kPa (12 in. H_2O) steady
Collector screen	15 kV, falling to 1 kV; 2 mA, rising to 5 mA
Inlet mass loading	62 mg/m^3
Mass removal efficiency	61%

There was good penetration of diesel soot through the fiberglass. However, this penetration caused the buildup of electrically

conductive paths. Electrification of the collector screen was impossible after one hour of operation.

Test 4:

The collector screen was biased positive, with the intent of enhancing agglomeration of particulate on the screen before re-entrainment. The outer grounded screen of the collecting section was lined with a 0.6 cm thick layer of Owens-Corning FM108 fiberglass filter material. The filter was not thick enough to be in contact with the high voltage screen. The test results are summarized below.

Mass sampling period	2 hours
Engine backpressure	3 kPa (12 in. H_2O) rising to 5 kPa (20 in. H_2O)
Collector screen	20 kV, falling to 12 kV; 1 mA, rising to 5 mA
Inlet mass loading	61 mg/m^3
Mass removal efficiency	41%

In this arrangement, a cake of diesel soot formed on the surface of the fiberglass, and gas sneakage past either end of the fiberglass cylinder ensued at 5 kPa backpressure. This gas sneakage led to heavy deposits of diesel soot on the teflon insulating and supporting plates at either end of the cylindrical collecting section. The buildup of diesel soot led to electrical failure of the collecting section after 2 hours operation.

Conclusions

One difficulty with the concept of a replaceable cartridge filter is exhaust gas sneakage around the edges of the filter. Gas sneakage will occur after a short operating period due to rising engine backpressure, as a result of a dense cake of diesel soot forming on the filter. In regard to electrification of the filter, any improvement in filtration due to the superimposed electric field is masked by electrical deterioration due to the buildup of diesel soot deposits. These two problems discourage further testing and practical development of this electrified filter.

ESP/CYCLONE COMBINATIONS

Three different series of tests were conducted to test the concept of using cyclonic collection of diesel particulate that had been agglomerated in the ESP. All tests were conducted with the diesel truck running at 88 km/hr (55 mph).

Fisher-Klosterman Industrial Cyclone

A Fisher-Klosterman XQ-4 industrial cyclone was connected in the exhaust line after the ESP. This cyclone was calibrated by the manufacturer under ambient conditions to have a D50 cut-point at 2.0 μm for a volume gas flow of 5 m^3/min (180 acfm). By Lapple's law, the D50 cutpoint extrapolates to 1.6 μm under the actual operating conditions (173°C, 2.5 x 10^{-5} pascal·sec, 6.2 m^3/min, 36.5 m/sec, and 108 kPa positive pressure (27 in. H_2O)).

Performance of the ESP/cyclone combination was tested by extracting samples of the exhaust gas through cascade impactors. Three test stations were used to accumulate data simultaneously at the outlets of the diesel truck, the ESP, and the cyclone. Cascade impactor data for the ESP/cyclone combination are shown in Figures 40 and 41. The data points represent averages of several independent measurements.

ESP Performance

The agglomeration of diesel particulate by the ESP is demonstrated in Figure 40, where the mmd at the ESP outlet is increased by roughly one order of magnitude to about 2.5 μm. (In regard to the curve labeled TRUCK OUTLET, note that the cascade impactor data do not give a reliable measurement of the mme in the very small size ranges of the primary diesel particulate. On the basis of electrical aerosol size analyzer data combined with cascade impactor data, the mmd of the primary diesel particulate is known to be approximately 0.3 μm.) The total mass loading of the impactor stages plus backup filter was 37.0 mg/scm at the truck outlet and 27.2 mg/scm at the ESP outlet. The ESP alone achieved about 26% mass removal efficiency.

The buildup of diesel soot on the collector cylinders of the ESP eventually caused excessive current in the collector circuit. During the tests of the ESP in combination with other devices, it was necessary to clean the collector cylinders by wet flushing with perchloroethylene after 16 to 20 hours of operation with the diesel truck running at 88 km/hr (55 mph).

Cyclone Performance

Figure 40 shows that about 56% of the diesel particles at the ESP outlet had aerodynamic diameter greater than 1.6 μm, the extrapolated D50 cutpoint of the cyclone. However, the total mass loading at the cyclone outlet was 34.7 mg/scm, 28% greater than at the ESP outlet. There was evidently substantial hydrocarbon condensation in the gas stream passing through the cyclone. The gas temperature dropped from 173°C to 163°C across the cyclone. The pressure differential was not large enough to measure on a mercury manometer.

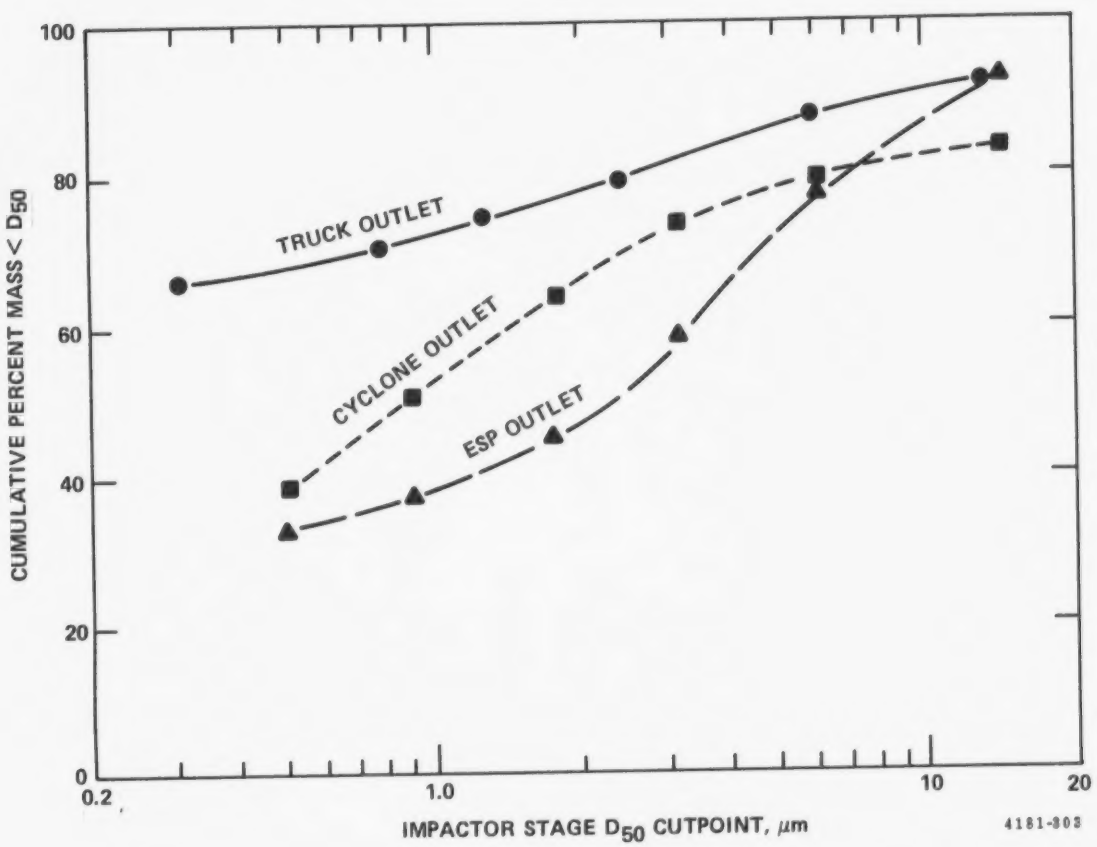

Figure 40. Impactor testing of ESP/cyclone combination. Cumulative percent particulate mass of aerodynamic diameter less than the impactor stage D_{50} cutpoints.

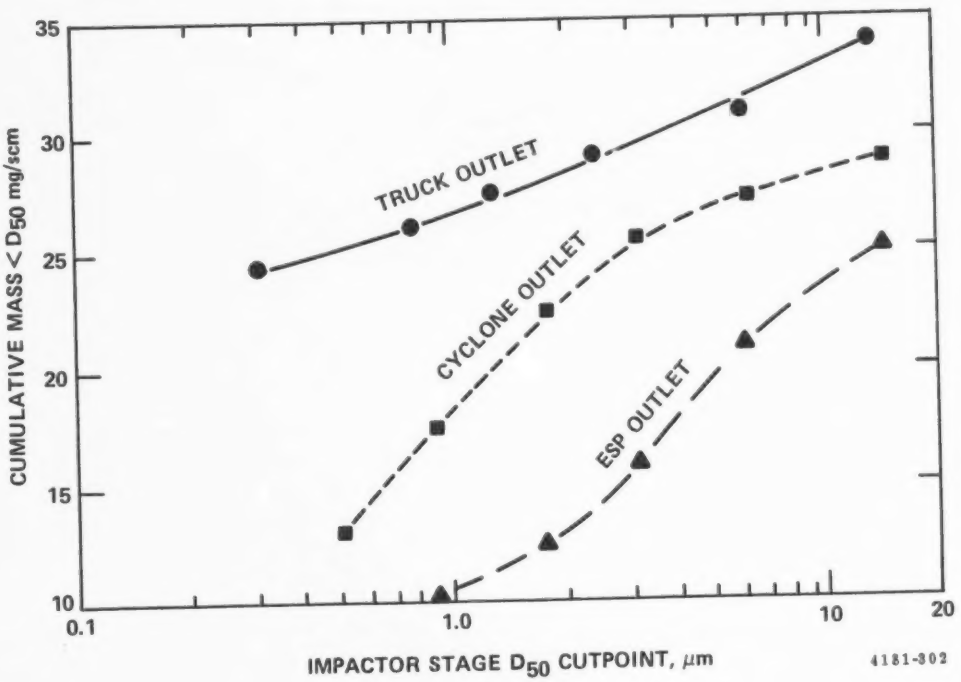

Figure 41. Impactor testing of ESP/gravel bed combination. Cumulative percent particulate mass of aerodynamic diameter less than the impactor stage D_{50} cutpoints.

Figure 40 shows also that the mmd of the diesel particulate was greatly reduced (to about 0.9 μm) in passing through the cyclone. This was not due to collection of large particles in the cyclone because only a very small amount of diesel soot was retained in the cyclone catchpot. The decrease in mmd could result both from hydrocarbon condensation and from breakup of the fluffy, agglomerated soot particles. Visual comparison of impactor stages from measurements before and after the cyclone clearly showed proportionately much heavier particulate loadings on the later impactor stages after the gas stream passed through the cyclone. It was not clear whether the breakup of agglomerated soot particles occurred in the vortex of the cyclone, in reentrainment from the cyclone catchpot, or in the impactor jets.

Five Stage Sampling Cyclone

After failing to trap the agglomerated carbon soot in the large industrial cyclone, the concept of an ESP/cyclone combination was tested further with a small five-stage cyclone system designed and calibrated for in situ stack sampling. In this case, a gas sample at the ESP outlet was extracted through the five-stage cyclone at 170°C and 0.03 m^3/min (1 acfm). The corresponding calibrated D50 cutpoints are 8.3, 3.9, and 2.5 μm for the first three cyclones, and an estimated 1.1 and 0.5 μm for the last two cyclones. A total of 136 mg of diesel particulate was collected in the cyclones (57%) and on the backup filter (43%). The measured mass distribution is displayed in Table 6. The five-stage cyclone data are compared with the cascade impactor data, where the cumulative percent mass of aerodynamic diameter greater than the D50 cutpoint is extracted from the ESP OUTLET curve of Figure 40. The five-stage sampling cyclone collects about the expected amount of agglomerated diesel particulate. This test indicates that an ESP/cyclone combination is a viable concept for aftertreatment of diesel exhaust.

TABLE 6. CUMULATIVE PERCENT MASS > D50 OF DIESEL SOOT AGGLOMERATED BY THE ESP

	8.3 μm	3.9 μm	2.5 μm	1.1 μm	0.5 μm
Cascade Impactors	17%	35%	49%	61%	67%
Five-Stage Cyclone	24%	35%	44%	50%	57%

Other Cyclone Combinations

Further tests were conducted on various combinations of sampling cyclones, with diesel exhaust gas samples (at the ESP outlet) pulled through the cyclones at much higher flow rates than that for which they were designed. The concept under investigation was that if such a cyclone could collect agglomerated diesel particulate efficiently at a flow rate of 0.55 to 0.85 m^3/min (20 to 30 acfm), then the total exhaust gas flow out of an ESP agglomerator could be passed through a parallel array of perhaps 10 such cyclones.

The tests were conducted with the diesel truck running at 88 km/hr (55 mph) and with cyclone sampling gas temperatures of approximately 170°C (340°F). The cyclone combinations were tested at flow rates of 0.55 and 0.80 m^3/min (20 and 28 acfm), the latter rate being the maximum capacity of the sampling pump. Particulate masses collected in the cyclone catchpot and in a backup filter were measured.

The three cyclones used were designated #9, #3, and #4, with specifications as follows:

Cyclone #9 - Large IP (inhalable particulate) Cyclone
D50 = 15 µm at 0.015 m^3/min, 22°C
D50 = 17 µm at 0.015 m^3/min, 170°C

Cyclone #3 - Small IP Cyclone (mounted inside Cyclone #9)
D50 = 2.5 µm at 0.015 m^3/min, 22°C
D50 = 2.9 µm at 0.015 m^3/min, 170°C

Cyclone #4 - Cyclone #4 of the Five-Stage Sampling Cyclone Series
D50 = 0.6 µm at 0.03 m^3/min, 22°C
D50 = 1.1 µm at 0.03 m^3/min, 170°C

Results of testing the cyclones at high flow rates are given in Table 7.

TABLE 7. SUMMARY OF TESTING SMALL CYCLONES AT HIGH GAS FLOW RATES

Test	Cyclone	Flow Rate m^3/min	Pressure Drop kPa (in. H_2O)	% Mass in Catchpot
1	9	0.55	1 (4)	23
2	9 and 3	0.55	56 (14)	52
3	9 and 3	0.80	96 (24)	52
4	4	0.80	96 (24)	37

Conclusions

An ESP agglomerator followed by cyclonic trapping of agglomerated particles is a viable concept for aftertreatment of diesel exhaust. The mass removal efficiency of such a device is at least 50%. The mass removal efficiency can be improved by extensive engineering and testing to match the cyclone performance to the characteristics of the agglomerated diesel particulate.

Methods for disposal of the trapped diesel soot require further investigation. An ESP will require cleaning sooner or later, by wet flushing or air jet scouring. Soot collected in the cyclone catchpot will have to be removed and/or compacted. The periodic maintenance of an ESP/cyclone combination appears unlikely to be a simple matter.

ESP/GRAVEL BED FILTER COMBINATION

The gravel bed filter, previously tested on primary diesel exhaust, was connected in the exhaust line after the ESP to test the concept of using a granular filter to trap diesel particles that had been agglomerated in the ESP. Three series of tests were conducted with different configurations of the gravel bed and at different diesel truck speeds.

Testing at Diesel Truck Speed 88 km/hr (55 mph)

As in previous testing, the gravel bed consisted of about 10 cm depth of 2 mm steel shot supported on a screen in a drum of diameter 45 cm (18 in.). Performance of the ESP/gravel bed combination was tested by extracting samples of the exhaust gas through cascade impactors. Three test stations were used to accumulate data simultaneously at the outlets of the diesel truck, the ESP, and the gravel bed.

Cascade impactor data for the ESP/gravel bed combination are shown in Figures 42 and 43. The data points represent averages of several independent measurements. The combination was tested with and without stirring of the surface of the gravel with a rake to break up the cake of carbon soot that forms on the surface. Stirring resulted in a large puff of collected carbon soot passing on through the exhaust line. The curves labeled "with stirring" represent average data for impactor runs which included one stir in the middle of each 30 minute data collection run. The curves labeled "without stirring" represent average data for runs taken over three days, with the gravel bed stirred once each day before the beginning of testing. This daily stirring typically reduced the engine backpressure from a maximum value of 17 kPa (68 in. H_2O) to about 12 kPa (48 in. H_2O). Comparison of data from afternoon impactor runs and runs the next morning, after stirring,

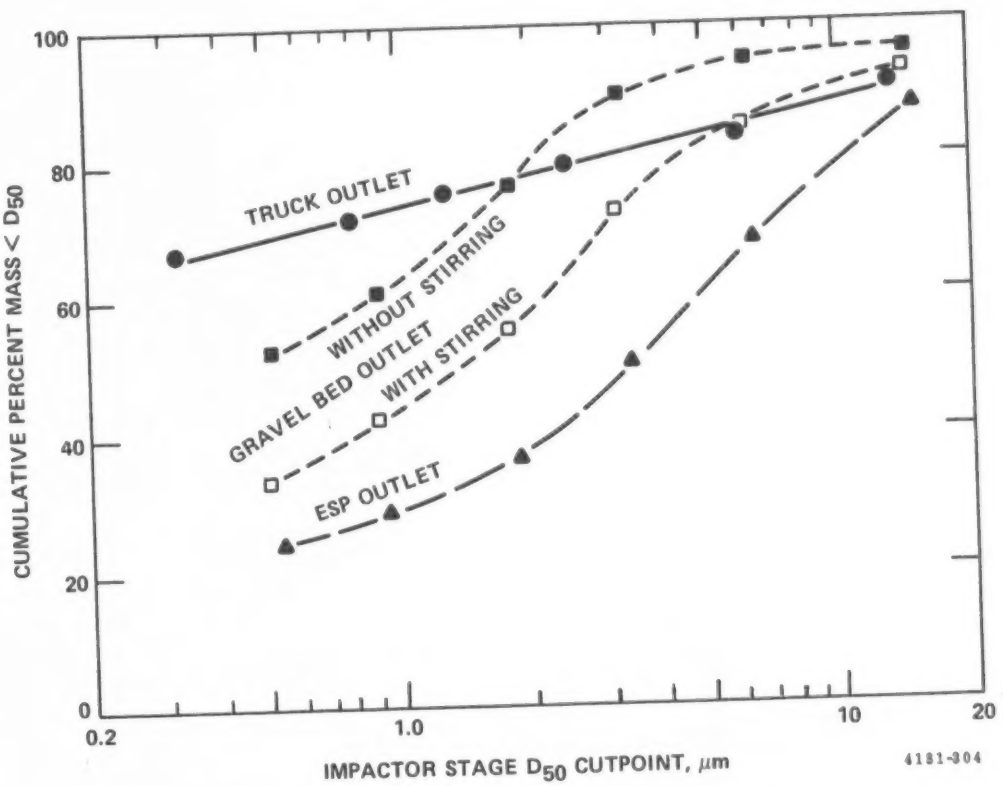

Figure 42. Impactor testing of ESP/gravel bed combination. Cumulative percent particulate mass of aerodynamic diameter less than the impactor stage D_{50} cutpoints.

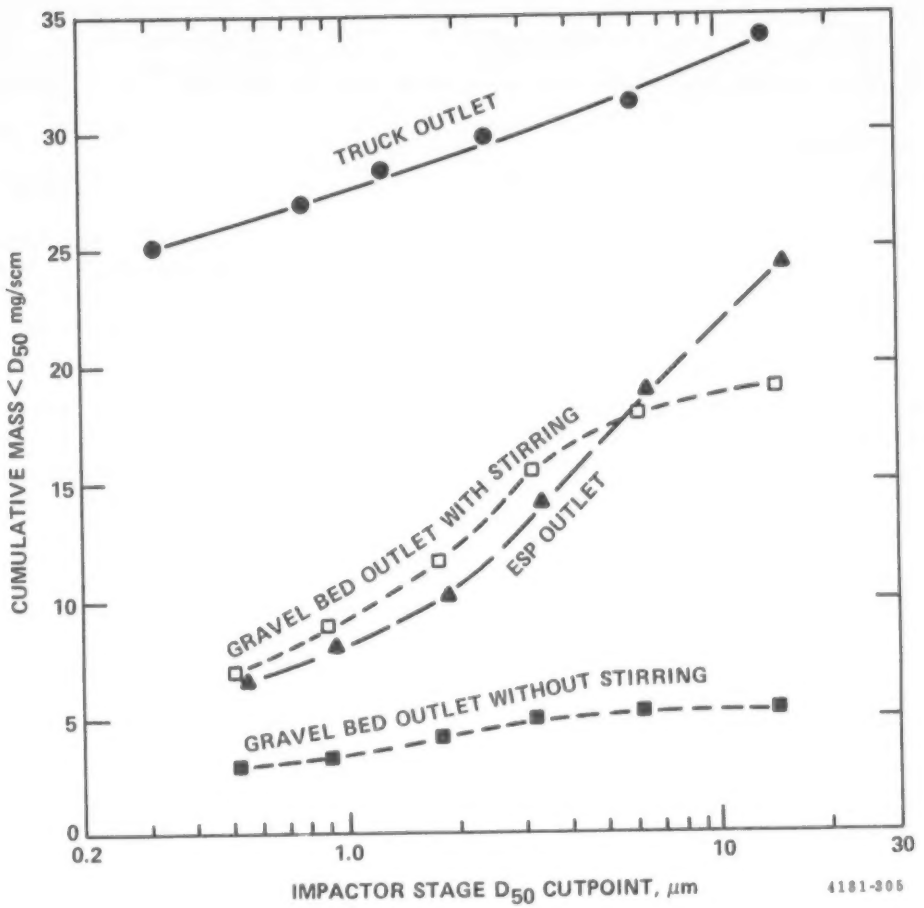

Figure 43. Impactor testing of ESP/gravel bed combination. Cumulative percent particulate mass of aerodynamic diameter less than the impactor stage D_{50} cutpoints.

indicated that the mass removal efficiency did not vary measurably with the change in engine backpressure.

TABLE 8. TOTAL MASS LOADINGS MEASURED FOR THE ESP/GRAVEL BED COMBINATION

Sampling Point	Total Mass Loading mg/scm	Total Removal Efficiency %
Truck Outlet	37.7	--
ESP Outlet	27.7	26
Gravel Bed Outlet		
with stirring during impactor runs	20.7	45
without stirring	5.4	86

The total mass loading of the impactor stages plus backup filter is summarized in Table 8. The ESP alone achieved about 26% mass removal efficiency, as in previous cascade impactor testing of the ESP/cyclone combination. The ESP had to be cleaned every 16 to 20 hours of operation at a diesel truck speed of 88 km/hr (55 mph). The overall mass removal efficiency, without stirring the gravel bed, was 86%. The data in Figure 42 show that the mmd of the agglomerated diesel soot (about 3.5 μm) is greatly reduced when the gas stream passed through the gravel bed. This is the result of larger particulate being trapped in the gravel bed.

Figure 44 shows electrical aerosol size analyzer data for the ESP/gravel bed combination, with the diesel truck running at 88 km/hr (55 mph). These data show the effect of treatment devices on the very fine particulate that is predominant in the primary diesel exhaust. In the aerodynamic size range around 0.1 μm, the ESP alone achieved 60 to 70% removal of particulate mass, consistent with the earlier EASA data, shown in Figure 35. The addition of the gravel bed resulted in only a small improvement in mass removal in this small size range. The main function of the gravel bed is to trap the particulate mass which has been shifted to a larger size range by the ESP.

Testing at Diesel Truck Speed 24 km/hr (15 mph)

The ESP/gravel bed combination was tested (without stirring) with the diesel truck running at 24 km/hr (15 mph). These tests

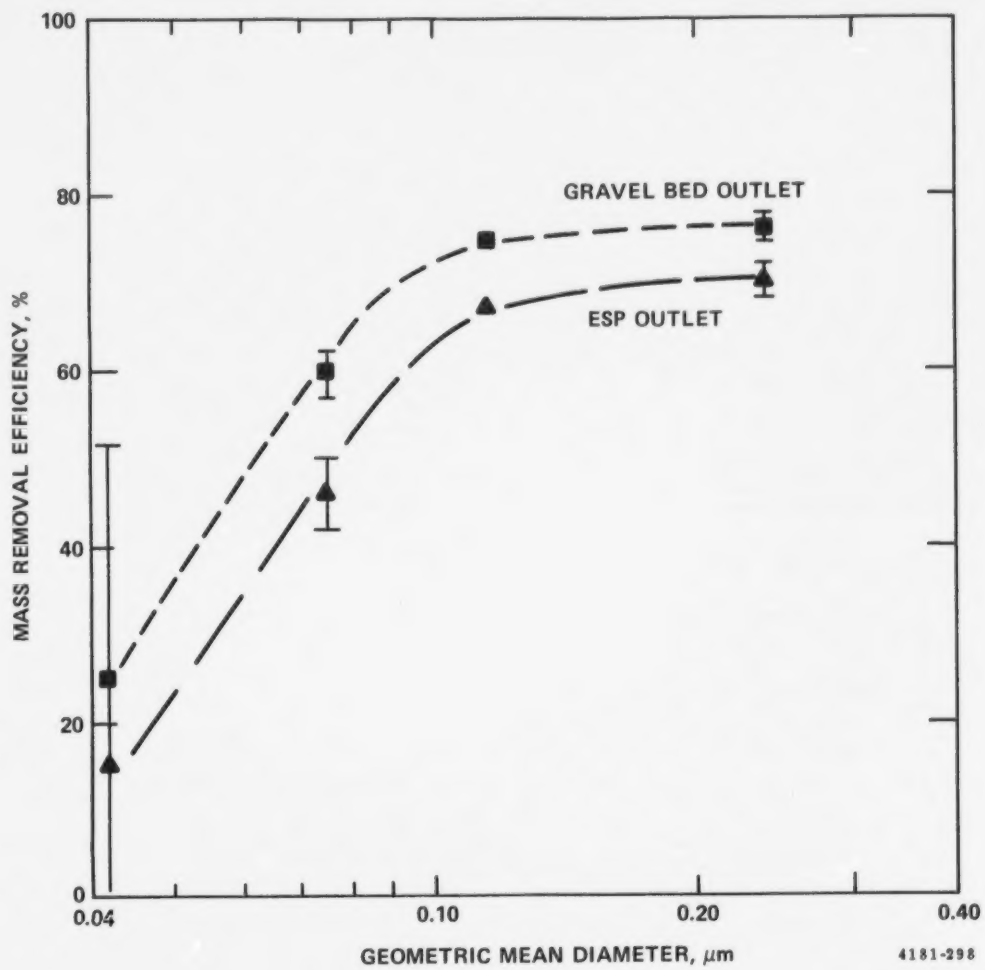

Figure 44. Mass removal efficiency in small size ranges of diesel particulate.

were intended to simulate lower speed conditions and smaller displacement engines. Cascade impactor measurements at the outlet of the gravel bed were found to be unreliable because the testing time had to be so long to accumulate measurable mass that the impactor substrate weight gain corrections were comparable to the mass collected. Consequently, mass train measurements at the gravel bed outlet were compared with total mass loadings from cascade impactor measurements at the diesel truck outlet. Throughout this series of tests the engine back-pressure remained steady at about 2.5 kPa (10 in. H_2O).

With the decrease in truck speed, the exhaust gas volume flow decreased from approximately 6.2 m^3/min (220 ACFM) to 2.2 m^3/min (80 ACFM) at 95°C (205°F). The particulate mass loading at the diesel truck outlet did not remain constant, but increased by roughly 75% to about 65 mg/scm. At the same time, the ESP/gravel bed combination collected more particulate mass per unit volume at the lower gas flow. The overall mass removal efficiency was 83%, about the same as at 88 km/hr (55 mph).

With the diesel truck running at 88 km/hr, the high gas flow past the corona electrode of the ESP kept the insulating standoff sufficiently clear of diesel soot that no cleaning of the corona section was ever required. At 24 km/hr, however, electrical failure of the corona electrode was experienced after about 10 hours of operation. Dry brushing of the diesel soot accumulated on the corona insulator restored normal electrical behavior.

Testing at Diesel Truck Speed 88 km/hr with a Smaller Gravel Bed

Because the ESP/gravel bed combination had demonstrated high-efficiency cleaning of diesel exhaust gas for a practical operating time, the gravel bed was reduced to a more practical size. A gravel bed diameter of 20 cm (8 in.) was chosen to correspond to the diameter of the ESP and to achieve a reduction in filter area by a factor of 5. The effect on mass removal efficiency was tested by mass train sampling at the diesel truck outlet and at the gravel bed outlet. Test results for gravel beds of depth 5 cm and 10 cm are summarized in Table 9. These tests were performed with the truck operating at 88 km/hr (55 mph) resulting in a filtration velocity of 3.2 m/sec.

Conclusions

The mass removal efficiency of an ESP/gravel bed combination used for diesel exhaust gas cleaning was largely independent of the running speed of the diesel vehicle. The higher mass loadings at lower exhaust gas flow rates were compensated by collection of greater particulate mass per unit volume gas flow by both the ESP and the granular filter. On the other hand, lower exhaust gas flow rates reduce the scouring of the insulating standoffs in the ESP. The periodic cleaning necessary for an ESP agglomerator

used on a diesel vehicle will possibly be more frequent for city driving than for long-distance highway driving.

TABLE 9. MASS REMOVAL EFFICIENCY OF THE ESP IN COMBINATION WITH 20 cm DIAMETER GRAVEL BED FILTER

Gravel Bed Depth cm	Engine Backpressure kPa (in. H_2O)	Outlet Mass Loading Truck mg/scm	Gravel Bed mg/scm	Efficiency %
5	10 (40) rising to 15 (60) in 3 hours	34.9	15.3	56
10	12 (48) rising to 16 (64) in 3 hours	37.9	11.6	69

A compact gravel bed filter can be contained within the housing of the ESP, directly below the collecting cylinders, and can achieve mass removal efficiency of 70%, or better, at acceptable levels of engine backpressure. The gravel bed filter can be cleaned simultaneously with the ESP by wet flushing with perchloroethylene.

ESP/DEEP BED FILTER COMBINATION

The deep bed filter, previously tested on primary diesel exhaust, was connected in the exhaust line after the ESP to test the concept of using a fiber filter to trap diesel particles that had been agglomerated in the ESP. The filter box (Figure 12) was loaded with a 8 cm thick batt of fiber glass thermal insulation. Particulate mass loadings at the diesel truck outlet and the filter box outlet were determined by mass train sampling, with the diesel truck running at 88 km/hr (55 mph).

During the first two hours of operation, the average mass loadings were 37.3 mg/scm at the diesel truck outlet and 11.2 mg/scm at the filter box outlet. The overall mass removal efficiency of the ESP/filter combination was 70%. If the mass removal efficiency of the ESP alone was 26% (based on previous cascade impactor measurements) then the efficiency of the deep bed filter acting on the agglomerated diesel particles was only 59%. During this testing time, the engine backpressure increased from 4.5 kPa (18 in. H_2O) and leveled off at 12 kPa (48 in. H_2O) after three hours of operation. After the backpressure leveled off, indicating gas sneakage around the edges of the fiberglass batt, the overall

mass removal efficiency dropped to 30%. At this point, the deep bed filter was contributing little to the overall efficiency. Visual inspection of the sooty deposits on the fiberglass batt after testing confirmed gas sneakage around the edges of the filter after the formation of a dense cake of diesel soot on the surface of the filter.

Conclusions

The agglomeration of diesel soot in the ESP did little or nothing to alleviate the problem of the diesel soot forming a cake on the surface of the filter rather than penetrating into the body of the filter. The ESP/filter combination exhibited the behavior common to all fiber filters tested: moderately high mass removal efficiency, but short lifetime due to rapidly rising engine backpressure.

SECTION 8

DESIGN OF AN AFTERTREATMENT DEVICE

Data from the laboratory experiments on aftertreatment of diesel exhaust have been used to design a prototype exhaust cleaning device. A schematic drawing of the proposed design concept is given in Figure 45. The device consists of an ESP agglomerator followed by a bed of steel shot to trap the agglomerated diesel particulate matter. A series of sharpened disc corona electrodes, similar to that tested in the electrified filter, are housed in the inlet exhaust pipe in order to minimize the overall size of the device. The ESP collecting section of concentric cylinders and the 20 cm diameter gravel bed are the same as those tested in this program. The overall length of the device is 84 cm (33 in.).

The design concept is based not on any theoretical efficiency calculations but rather on the data from the actual laboratory testing of the components. The overall mass removal efficiency of the device is at least 70%. The duty period is at least 16 hours, for diesel soot loadings similar to those measured for the test vehicle. In the duty period, the engine backpressure is expected to remain below 25 kPa (100 in. H_2O). The device is designed to be operated in a vertical orientation and cleaned by wet flushing with perchloroethylene. The device is suitable for use on stationary diesel engines or on large, heavy-duty diesel vehicles engaged in fleet operation where periodic maintenance can be performed at a central garage.

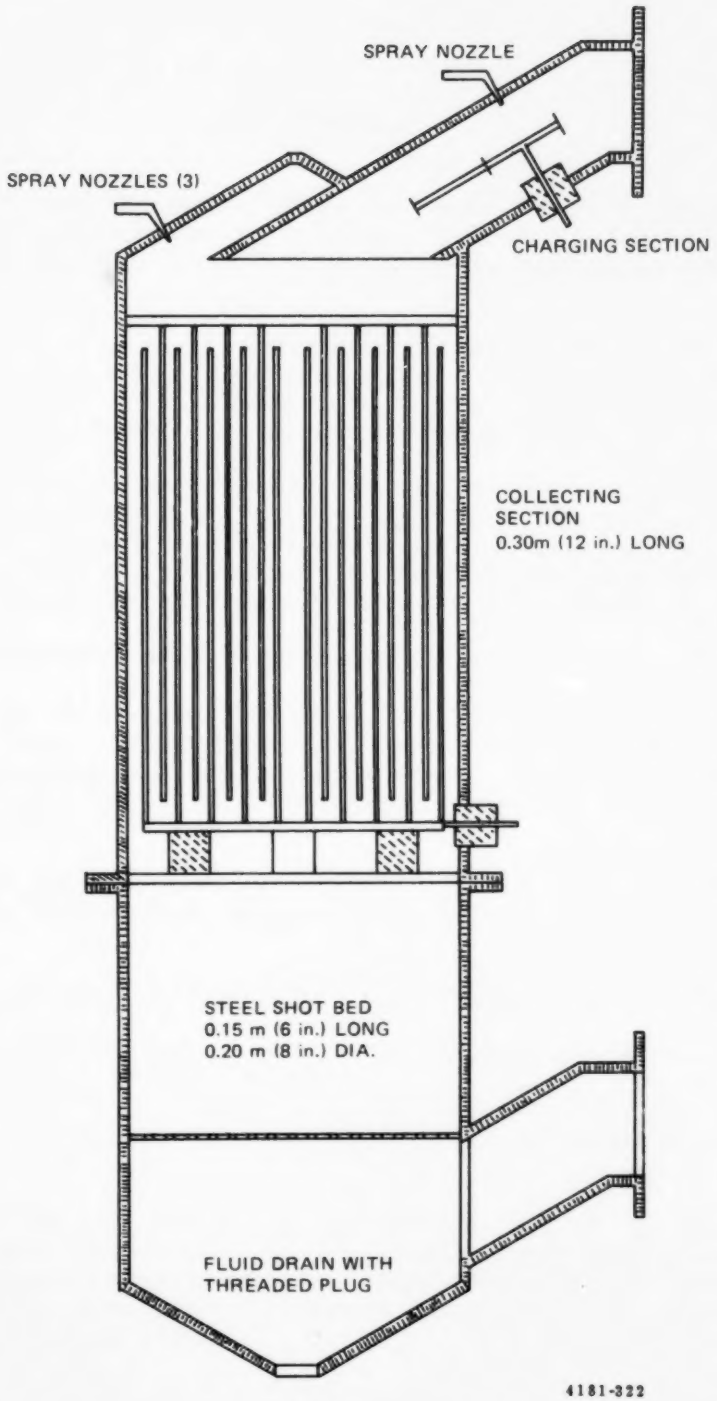

Figure 45. Schematic diagram of prototype diesel exhaust cleaning device. Minimum collection efficiency 70%. Overall length 0.84 m (33 in.).

REFERENCES

1. Frey, J. W. and M. Corn. Physical and Chemical Characteristics of Particulates in a Diesel Exhaust. American Industrial Hygiene Association Journal, September-October, 1967.

2. McCain, J. D. and M. G. Faulkner. Assessment of Diesel Particulate Control: Particle Size Measurements. EPA-600/7-79-232C (NTIS PB80-224256), U.S. EPA, IERL, Research Triangle Park, North Carolina, December 1979.

3. Lipkea, W. H., J. H. Johnson, and C. T. Vuk. The Physical and Chemical Character of Diesel Particulate Emissions - Measurement Technique and Fundamental Considerations. SAE Paper #780108, presented at the SAE Congress and Exposition, Detroit, Michigan, February 27 - March 3, 1978.

4. Federal Register, 44(33) February 1, 1979.

5. Faulkner, M. G., E. B. Dismukes, J. R. McDonald, D. H. Pontius, and A. H. Dean. Assessment of Diesel Particulate Control: Filters, Scrubbers, and Precipitators. EPA-600/7-79-232a (NTIS PB80-128655), U.S. EPA, IERL, Research Triangle Park, North Carolina, October 1979.

6. Ranz, W. E. and J. B. Wong. Impaction of Dust and Smoke Particles. Industrial Engineering Chemistry, 44(6):137-138, 1952.

7. Davies, C. N. and M. Aylward. Proc. Phys. Soc., (64):889, 1951.

8. Marple, W. A. Doctoral Thesis, University of Minnesota, Minneapolis, MN, 1970.

9. Rao, A. K. Doctoral Thesis, University of Minnesota, Minneapolis, MN, 1975.

10. Cushing, K. M., G. Lacey, J. D. McCain, and W. S. Smith. Particulate Sizing Techniques for Control Device Evaluation: Cascade Impactor Calibrations. EPA-600/2-76-280 (NTIS PB-245184), U.S. EPA, IERL, Research Triangle Park, North Carolina, October 1976.

11. Harris, D. B. Procedures for Cascade Impactor Calibration and Operation in Process Streams. U.S. EPA Report No. EPA-600/2-77-004, January 1977.

12. Felix, L. G., G. I. Clinard, G. E. Lacey, and J. D. McCain. Inertial Cascade Impactor Substrate Media For Flue Gas Sampling. Interagency Energy-Environment Research Development Program Report, EPA-600/7-77-060, June 1977.

13. Hewitt, G. W. The Charging of Small Particles for Electrostatic Precipitation. Transaction AIEE, 76:300-306, 1957.

14. Liu, B. Y. H., K. T. Whitby, and D. Y. H. Pui. A Portable Electrical Aerosol Analyzer for Size Distribution Measurements of Submicron Aerosols. APCA J. 24(11):1067-72, 1974.

15. Liu, B. Y. H. and D. Y. H. Pui. On the Performance of the Electrical Aerosol Analyzer. J. Aerosol Science, 6:249-64, 1975.

16. Sem, G. J. Submicron Particle Sizing Experience on a Smoke Stack Using the Electrical Aerosol Size Analyzer. Seminar - In-Stack Particle Sizing for Particulate Control Device Evaluations. EPA-600/2-77-060, U.S. EPA, IERL, Research Triangle Park, North Carolina, 1975.

17. Ragland, J. W. Measurement of Ultrafine Particle Size Distributions in Industrial Flue Gases Using an Electrical Aerosol Analyzer. Aerosol Measurement, Lundgren, D. A. et al, eds. University Presses of Florida, Gainesville, Florida, 1979.

18. Cushing, K. M. and W. B. Smith. Procedures Manual for Fabric Filter Evaluation. EPA-600/7-78-113, U.S. EPA, IERL, Research Triangle Park, North Carolina, 1978.

19. Liu, B. Y. H. and A. Kapadia. A Computer Data Reduction Program for the Electrical Aerosol Analyzer. PTL Pub. No. 325. University of Minnesota, Particle Technology Laboratory, Minneapolis, Minnesota, 1977.

20. Personal communication from S. Masuda to J. R. McDonald, Southern Research Institute.

GLOSSARY

Aerodynamic diameter: The diameter of a sphere of unit density which has the same settling velocity in the gas as the particle of interest.

Agglomerated particles: Particles which have stuck together to form a larger particle.

Backpressure: Pressure difference between the engine's exhaust pipe and ambient air.

Barrier filter: A type of filter in which the gas has to pass through a porous wall.

Cyclone: A device that causes an aerosol to spiral around its walls, thus separating particles by centrifugal action.

D_{50}: The particle diameter at which a collection device is 50 percent efficient.

Dynomometer: A device for measuring the power of an engine.

Filter blinding: The covering of the front surface of a filter by an impenetrable cake of collected particles.

Filter velocity: The gas velocity through the filter material.

Gas sneakage: The bypassing of the collection region by the gas.

Isokinetic sampling: A gas sampling condition in which the gas in the inlet to the sampling tube has the same velocity as the gas outside the tube.

Reentrainment: Loss of collected particles back into the gas stream.

Regenerative device: A device which cleans itself of accumulated material, frequently by combustion.

Sintered metal: Metal which is fused together for greater rigidity.